

AN INVESTIGATION OF THE DEGREE OF FORBIDDENNESS IN
COMPLEX β -DISINTEGRATION USING THE METHOD OF $\beta - \gamma$
ANGULAR CORRELATION

Thesis

Submitted by

ROGER D. SCOTT, B.Sc.

for the degree of

DOCTOR OF PHILOSOPHY

University of Edinburgh

November, 1967.



C O N T E N T S

	Page
 <u>CHAPTER 1</u>	
1.1 Introduction to the Angular Correlation Method	1
1.2 Historical Survey	4
1.3 The Information Available from Angular Correlation Experiments	8
1.4 The Problem under Investigation	11
 <u>CHAPTER 2</u>	
2.1 Elementary Theory of Angular Correlations	14
2.2 Limitations of the Elementary Theory	17
2.3 The Density Matrix Formalism	18
2.4 The Density Matrix Description of the Angular Correlation Process	22
2.5 The Theory of β Decay	26
(a) Introduction	26
(b) The β decay Interaction	27
(c) Recent Developments of the Theory	29
(d) The Allowed Transitions	31
(e) The Forbidden Transitions	33
(f) Coulomb Corrections: The "Normal" and " ξ " Approximations	34
(g) The Energy Spectrum and $\log ft$ Values	36
(h) The β - γ Angular Correlation	39

C O N T E N T S (Contd.)

Page

CHAPTER 3

3.1	The Angular Correlation Chamber	42
3.2	The Source Holder	43
3.3	The β and γ Detectors	43
3.4	The Electronics	44
3.5	β and γ Spectra	44
3.6	Choice and Measurement of Coincidence Resolving Time	46
3.7	Preparation and Mounting of Sources	47

CHAPTER 4

4.1	Source Centring	53
4.2	Experimental Procedure	54
4.3	Treatment of Data	58
4.4	Geometrical and Other Corrections	67
	(a) β Back Scatter	70
	(b) Scattering of β Particles in the Source and Source Backing Material	71
	(c) β -Bremsstrahlung Angular Correlation	72
	(d) Perturbation	73
4.5	Results of the Angular Correlation Measurements	75

C O N T E N T S (Contd.)

Page

CHAPTER 5

5.1	The Decay Scheme of the Thorium Active Deposit	83
5.2	Predictions of the Nuclear Shell Model .	88
5.3	Conclusions	95

Acknowledgements

Appendix	98
References	99

CHAPTER 1

1.1 Introduction to the Angular Correlation Method

The excited states of nuclei are characterized by their energy relative to the ground state, by values of total angular momentum, commonly called spin, and parity. Such states may possess other attributes decided, perhaps, on the basis of some nuclear model but these are of no immediate concern in the description of this work. Decay to the ground state occurs by emission of radiation, usually γ rays or internal conversion electrons, and this de-excitation may take place in one step or via a series of intermediate levels. The latter process gives rise to a set of radiations in cascade. The ground state so reached may itself be unstable and decay in turn by particle emission to some state of the daughter nucleus where the process of de-excitation will again take place.

Information as to the spin, parity and energy of a nuclear level must be obtained by examining the properties of any radiation leading to or from that level. Thus, the energy of a level can be deduced from measurement of the energies of the radiations from that level, but this alone will not suffice to determine the spin and parity of the level. Other properties of the de-exciting radiations must be examined before spin and parity values can be assigned and, as the name implies, the angular correlation method makes use of the directional properties of radiations for

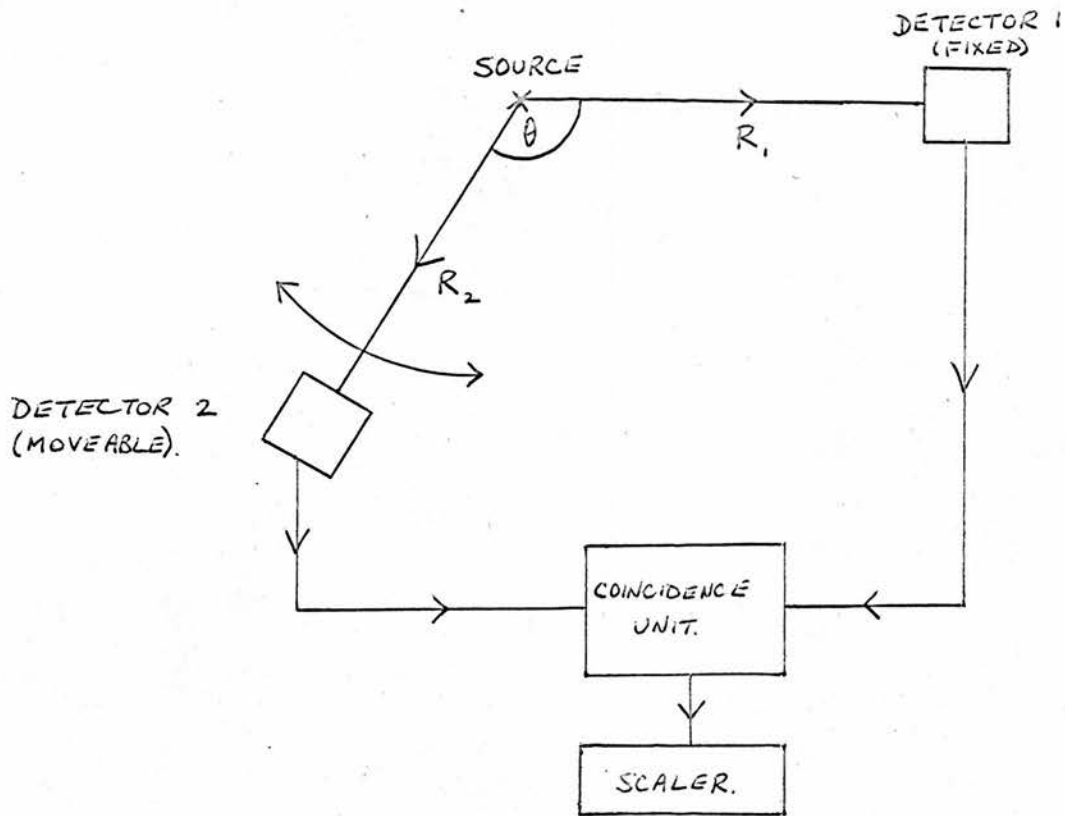


FIGURE 1.

this purpose.

Consider a decay where two radiations, R_1 and R_2 , are emitted in cascade and let the initial, intermediate, and final levels have spin and parity values $I_i \pi_i$, $I \pi$ and $I_f \pi_f$ respectively. The coincidence rate can be determined as a function of the angle θ between the radiations by using the experimental arrangement shown in Figure 1. Detector 1 detects R_1 only and detector 2 detects R_2 only. Since detector 1 is fixed, R_1 is observed in a fixed direction but detector 2 can be rotated about the source thus varying the angle θ between the radiations. The coincidence rate so determined as a function of θ may then be used to derive an angular correlation function, usually denoted as $W(\theta)$, and defined as the probability of observing R_2 at an angle θ to R_1 .

It is perhaps surprising at first sight that the coincidence rate should depend on θ at all since the radiation from a source where no attempt has been made to produce spin alignment is isotropic. However, the facts that the radiations are in cascade and that one of them is observed in a fixed direction produce a situation analogous to spin alignment, as the following argument shows. It is convenient to focus attention on γ emission but arguments of a similar nature can be used for any type of radiation.

γ ray emission is characterized by its multipole

order, that is by the quantity of angular momentum, in units of \hbar , carried away by the γ ray. A multipole transition of order (ℓ, m) will connect an initial state (I_i, M_i) to a final state (I_f, M_f) where

$$|I_i - I_f| \leq \ell \leq I_i + I_f$$

$$\text{and} \quad m = M_i - M_f \quad .$$

Here, ℓ , I_i and I_f are values of total angular momentum and m , M_i and M_f refer to their projections on some quantization axis. Thus, the possible values of m are $-\ell, -\ell+1, \dots, \ell-1, \ell$. Parity is conserved so that

$$\pi_i = \pi_f \pi_R$$

where π_R is the parity of the radiation field. The multipole radiation may be of electric or magnetic (E or M) type, the distinction being that the parity of an electric multipole field (ℓ, m) is $(-)^{\ell}$ and that of a magnetic multipole field (ℓ, m) is $(-)^{\ell+1}$. Hence in any given transition only certain combinations of multipole transitions can occur.

For a given value of ℓ , the angular distribution of quanta depends only on $m = M_i - M_f$ and so the probability of emission of a γ -ray depends on the angle between the arbitrary quantization (or z) axis and the direction of emission. A radioactive source having all

magnetic substates M equally populated for any arbitrary z axis (i.e. with nuclei randomly orientated) therefore gives an isotropic radiation distribution and hence if the angular correlation is to exist, there must also exist a non random distribution of spin orientations. If the arbitrary z axis is now chosen to lie along the fixed direction of observation of R_1 then the magnetic sub-levels of the intermediate state are no longer randomly populated, but are populated according to the different transition probabilities for each of the possible transitions M_1 to M . Hence the observation of R_1 in a fixed direction selects an ensemble of nuclei having non randomly orientated spins and the radiation from such an ensemble is not, in general, isotropic. This demonstrates the existence of an angular correlation.

The function $W(\theta)$ can be computed theoretically for any combination of nuclear spins and angular momentum carried off (by any type of radiation) and the angular correlation method is therefore a very powerful tool of nuclear spectroscopy.

1.2 Historical Survey

The initial suggestion that two successively emitted radiations might show an angular correlation was made by Dunworth and Price⁽¹⁾ in a paper by Dunworth on the application of coincidence techniques to experimental

nuclear physics. The idea was developed by Hamilton⁽²⁾ who was the first to produce a theory of the process. Hamilton's calculations applied to free nuclei, the possible effects on the correlation of any extra-nuclear perturbing fields being ignored. The lack of success in detecting any correlation in the early experiments of Beringer⁽³⁾ and Good⁽⁴⁾ was attributed to a masking of the correlation by magnetic coupling between the nucleus and the atomic electrons. Such coupling would cause transitions between the individual magnetic sub-levels of the intermediate state, provided the life time of that state was long enough, thus tending to restore the equal population of the sub-levels and destroying the correlation. Accordingly, Goertzel⁽⁵⁾ generalized the theory to take the influence of extra-nuclear fields into account. This perturbation effect might have explained negative experimental results in some cases, but it seems more likely that the experimental techniques were at fault since Geiger counters of low efficiency were used as γ detectors. The first successful correlation was performed by Brady and Deutsch⁽⁶⁾, using Geiger counters. The advent, at about this time, of scintillation counters with much higher efficiency solved the main experimental problem in the performance of such experiments.

Efforts were also made to generalize the theory of angular correlation so that it could be applied to the case of any radiation of arbitrary multipole order.

Hamilton had shown that, for cascades of either pure dipole or quadrupole radiations,

$$W(\theta) = 1 + a_2 \cos^2 \theta + a_4 \cos^4 \theta$$

where a_2 and a_4 were calculable for given spin sequences. Further development of the theory was a result of the application of group theory, Racah algebra and the density matrix formalism to the problem.

Yang⁽⁷⁾ proved some general statements about the form of $W(\theta)$ using group theory. He predicted the highest power of $\cos \theta$ to be expected from a given spin sequence. Thus, if the correlation is expressed as a sum of (even) powers of $\cos \theta$:

$$W(\theta) = 1 + \sum_{k=1}^{k_{\max}} a_{2k} \cos^{2k} \theta$$

$$\text{then } 0 < 2k < \text{Min}(2I, 2\ell_1, 2\ell_2) ,$$

for the case of pure radiations, where I is the spin of the intermediate state and ℓ_1 and ℓ_2 are the multipole orders of the two radiations. If the spin values of the states are such that multipole mixtures are allowed by the selection rules, then

$$0 < 2k < \text{Min}(2I, \ell_1 + \ell_1', \ell_2 + \ell_2') .$$

However, the calculations for a_{2k} involved summations which could not be performed in closed form.

Gardner⁽⁸⁾ then showed that the coefficients A_{2k} could be given in closed form provided that $W(\theta)$ was developed as a series of Legendre Polynomials:

$$W(\theta) = 1 + \sum_{k=1}^{k_{\max}} A_{2k} P_{2k}(\cos \theta) .$$

The A_{2k} then involved a summation over the products of Clebsch-Gordan coefficients which could be performed using Racah techniques. It was also shown that A_{2k} could be split up into two parts, one depending on each transition of the cascade.

A large amount of theoretical work was done on the problem in the late 1940's and early 1950's culminating in the comprehensive review article of Biedenharn and Rose⁽⁹⁾ which presents the theory in a complete and elegant form. Provided that suitable functions are used for the development of the angular correlation expression, it is possible to find closed forms for the coefficients of the expansion for arbitrary particles, multipole mixtures and polarizations. Furthermore, with very slight modifications, the theory may be used to describe angular distributions of particles arising from nuclear reactions. Reviews of the subject are also given by Devons and Goldfarb⁽¹⁰⁾, Frauenfelder and Steffen⁽¹¹⁾ and in Ferguson's book⁽¹²⁾. A brief account of the theory is presented in Chapter 2.

1.3 The Information Available from Angular Correlation Experiments.

Angular correlations can be performed using any two successively emitted radiations and, as the theory will show, the functional dependence of W on the angle θ is always the same, namely the Legendre polynomial $P_n(\cos \theta)$. However, the information which can be deduced about the nuclear levels depends on the type of radiation observed. Some typical experiments are discussed below.

(a) γ - γ Angular Correlations

This experiment is capable of yielding spin values but not the relative parities of levels. Relative parity values are not obtained because electric and magnetic multipole radiations of given (ℓ, m) have the same angular dependence. The transformation of electric to magnetic multipole field ($\underline{E} \rightarrow \underline{H}$, $\underline{H} \rightarrow -\underline{E}$) leaves the Poynting vector, and therefore the radiated energy distribution, unaltered. The correlation is sensitive to the mixing of multipoles in a transition, for instance $E2 + M1$ or the much rarer $E1 + M2$. Since the amplitude mixing ratio of the transition is involved, this is a more sensitive method of mixture detection than internal conversion measurements which are intensity measurements and as such depend on the square of the perhaps very small amplitude mixing ratio.

Relative parities can be determined if, in addition to the angular correlation, the direction of the electric vector of a γ ray, i.e. its polarization, is measured. The polarizations of E and M multipoles of order (l, m) are at right angles to one another. Polarization is usually measured by Compton scattering, since the differential cross-section for this process depends on the angle between the direction of polarization of the incident γ ray and the plane of scattering.

(b) γ -Conversion Electron Angular Correlations

The internal conversion process is sensitive to the multipolarity of a transition and also to the electric or magnetic nature of the transition. Relative parities may therefore be decided and this correlation is capable of supplying more information than the γ - γ correlation. Clearly the technique is essential if one or other of the γ rays is strongly converted, since it may not then be possible to perform a γ - γ correlation.

Internal conversion calculations taking account of finite nuclear size depend to some extent on the nuclear model used and, for high Z values, the finite nuclear size might influence the angular correlation. The angular correlation might, under the right circumstances, provide some information on nuclear structure.

In general, if x is an arbitrary radiation and both the γ - x and conversion electron - x angular correlations are possible, then the latter experiment yields

additional information on parity and possibly on nuclear structure.

(c) α - γ Angular Correlations

Level spins and the multipole orders of transitions are obtained from an α - γ angular correlation. Since the α particle has zero spin, the selection rules governing the multipole order of the α radiation in any transition are particularly simple. If ℓ , the orbital angular momentum, of the α particle is even, the states connected by the transition have the same parity and they have opposite parities if ℓ is odd. The correlation is therefore parity sensitive.

(d) β - γ Angular Correlations

Such experiments may yield spin values and information concerning the matrix elements involved in the β -decay. This matter is discussed in detail in Chapter 2 and it is sufficient to comment here that allowed β decays should give no angular correlation whereas forbidden decays are expected to show some anisotropy. Thus the β - γ angular correlation can be used as a test of degree of forbiddenness of a β transition.

It should be pointed out that none of the above experiments need necessarily produce unambiguous spin values of the nuclear levels involved in the transitions. It very often happens that the theoretical predictions

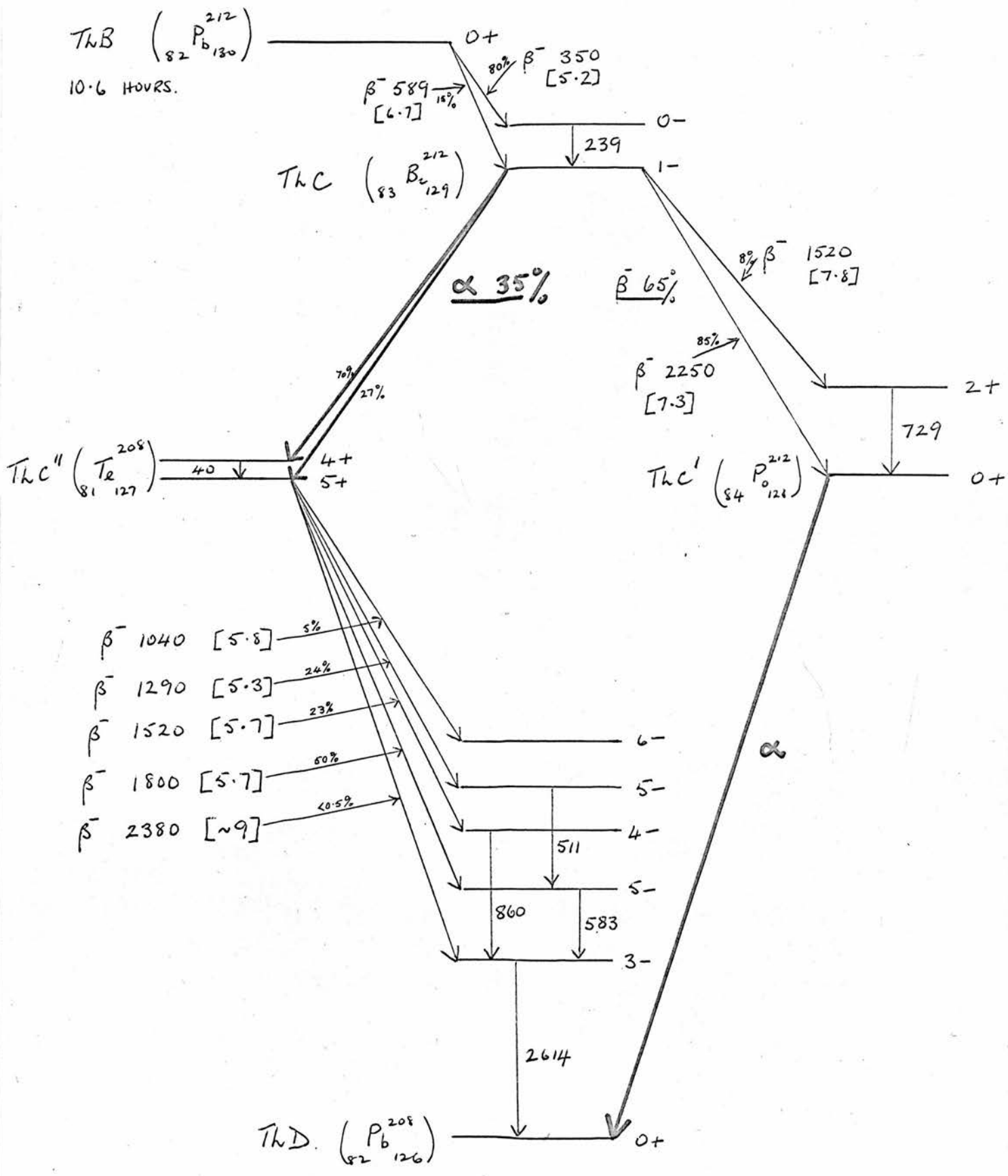


FIGURE 2

regarding two or more different cascades may lie so close together that it is impossible to distinguish the various possibilities experimentally by this means. In addition, the presence of small multipole mixtures might complicate conclusions drawn from experimental results, and perturbations caused by extra-nuclear fields are capable of reducing a correlation considerably, or even of wiping it out completely, if the physical nature of the source and the intermediate level life time are badly chosen.

1.4 The Problem under Investigation

$\beta - \gamma$ angular correlations have been performed using sources of the thorium active deposit with a view to determining the degree of forbiddenness of some of the complex β disintegrations occurring in the decay chain. Figure 2 shows the main features of the currently accepted decay schemes of the chain. In Figure 2, energies are quoted in keV and the figures in square brackets after the β^- energies are the calculated log ft values of the transitions. The meaning and significance of the quantity "log ft" is discussed in the section on β -decay theory in Chapter 2, but it may be noted at this point that the log ft value provides an indication of the degree of forbiddenness of a β transition and that certain of the transitions occurring in the thorium decay scheme are anomalous in this respect. Specifically, the 350 keV $0^+ \rightarrow 0^-$ transition in the ThB and all but the (very weak) highest energy transition in the ThC" \rightarrow ThD decay have log ft values

considered appropriate to allowed decays whereas, if the decay scheme of Figure 2 is accepted, all the β decays are seen to be first forbidden. The $\text{ThC} \rightarrow \text{ThC}'$ β decays have $\log ft$ values in keeping with their assignment as first forbidden transitions.

In an attempt to check the various spin and parity assignments, β - γ angular correlations have been performed using

- (a) the 350 keV β feed to the 0- level of ThC and the following 239 keV γ ray (the F line),
- (b) the 1800 keV β feed to the first 5- level of ThD and the 583 keV γ ray,
- (c) the 1520 keV β feed to the first excited state of ThC' and the 729 keV γ ray.

An attempt was also made to repeat the angular correlation reported by Demichelis and Ricci⁽¹³⁾ using the highest energy β transition occurring in the $\text{ThC}'' \rightarrow \text{ThD}$ decay, which feeds the first excited 3- level of ThD, and the 2614 keV γ ray.

A critical discussion of the spin and parity assignments of the complete decay scheme in the light of this and previous work is presented in Chapter 5.

A β - γ angular correlation was also performed using a source of E_u^{152} in order to test the apparatus used in this work by comparison of the result with those obtained by several investigators of this decay. The relevant part of the decay scheme is shown in Figure 3. The

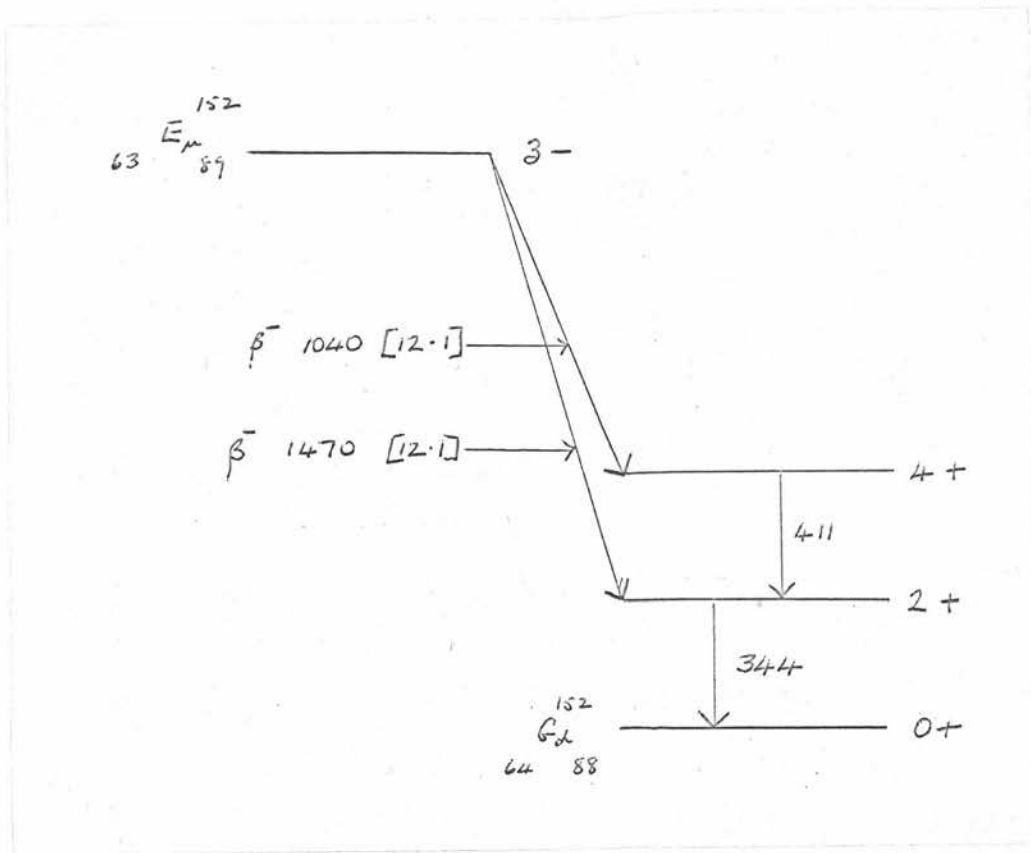


FIGURE 3.

correlation was performed using β particles of energy greater than 1 MeV in coincidence with the 344 keV γ ray.

The $\log ft$ values of the β decays in this scheme are seen to be abnormally high, considering that the decays are first forbidden according to the accepted spin and parity assignments. The theoretical explanation of such $\log ft$ values involves assumptions as to the relative sizes of the various matrix elements contributing to the decay and, experimentally, such decays afford an opportunity of measuring the sizes of the matrix elements rather than merely the ratios of certain linear combinations of matrix elements, as is usually the case.

CHAPTER 2

2.1 Elementary Theory of Angular Correlations

A γ -ray transition between two nuclear states having spins I_1, I and magnetic sub levels M_1, M respectively is made up of a number of experimentally unresolved components, each component arising from some particular transition $M_1 \rightarrow M$. Each of these components has an angular distribution $F_{\ell_1}^{m_1}(\theta)$, say, where θ is the angle between some arbitrary z-axis and the direction of emission, and the possible values of ℓ_1 and m_1 are governed by the angular momentum conservation rules, namely

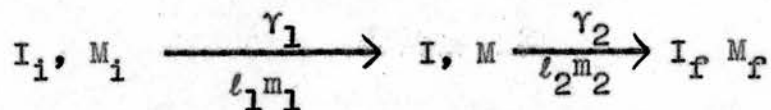
$$I_1 = I + \ell_1, \quad M_1 = M + m_1$$

The totality of unresolved transitions $M_1 \rightarrow M$ between the two states is referred to as a complete line. The directional distribution of a complete line $F_{\ell_1}(\theta)$ can be written

$$F_{\ell_1}(\theta) \propto \sum_{M_1 M} P(M_1) G(M_1 M) F_{\ell_1}^{m_1}(\theta)$$

where the $P(M_1)$ are the relative populations of the M_1 and the $G(M_1 M)$ are the relative transition probabilities of each transition $M_1 \rightarrow M$.

The angular correlation function, $W(\theta)$, can now be deduced for the case of a γ - γ cascade of the type



by selecting the quantization axis to coincide with the direction of emission of the first γ ray. For then $W(\theta)$ is simply the directional distribution $F_{\ell_2}^{m_2}(\theta)$ of the second γ ray with respect to this z-axis.

Thus

$$W(\theta) = F_{\ell_2}^{m_2}(\theta) \propto \sum_{MM_f} P(M) G(MM_f) F_{\ell_2}^{m_2}(\theta) .$$

$P(M)$ is given by the sum of all the transitions $M_i \rightarrow M$ and therefore, assuming the M_i to be equally populated,

$$P(M) \propto \sum_{M_i} G(M_i M) F_{\ell_1}^{m_1}(0) .$$

Thus

$$W(\theta) \propto \sum_{M_i MM_f} G(M_i M) F_{\ell_1}^{m_1}(0) G(MM_f) F_{\ell_2}^{m_2}(\theta) .$$

The absolute transition probability of a transition $M_i \rightarrow M$ is proportional to the square of the matrix element of some operator, in general a tensor operator. The Wigner-Eckart theorem (see, for example, reference (14)) enables such a matrix element to be written as the product of a geometrical factor and a scalar nuclear factor. The geometrical factor depends explicitly on M_i and M , but the nuclear factor is independent of these quantum numbers and is called the reduced matrix

element. The geometrical factor is the Clebsch-Gordan coefficient for the vector addition

$$\underline{I}_i = \underline{I} + \underline{\ell}_1, \quad M_i = m_1 + M$$

and so
$$G(M_i M) \propto \left[C_{IM \ell_1 m_1}^{I_i M_i} \right]^2$$

where C denotes the Clebsch-Gordan coefficient.

A further simplification is introduced by the special choice of z-axis. The γ ray photon is a spin 1 particle of zero rest-mass and the possible values of m_1 are therefore confined to ± 1 .

Hence

$$W(\theta) \propto \sum_{M_i M M_f} \left[C_{IM \ell_1 \pm 1}^{I_i M_i} \right]^2 F_{\ell_1}^{\pm 1}(0) \left[C_{I_f M_f \ell_2 m_2}^{I M} \right]^2 F_{\ell_2}^{m_2}(\theta) .$$

The Clebsch-Gordan coefficients are tabulated and the calculation of $F_{\ell}^m(\theta)$ for γ rays is a well known problem of classical electromagnetic theory. Thus $W(\theta)$ can be worked out for the case of γ - γ angular correlations involving pure multipoles without difficulty, although the summations become tedious if high spin values are involved in the cascade.

$W(\theta)$ has been derived in a form where the probabilities of each transition appear independently. In other words, the summation over the intermediate M values has been done incoherently so that the various possible ways in which a nucleus can decay from a given

initial state M_i to a given final state M_f are assumed to be independent. If the summations in the expression for $W(\theta)$ were performed before, rather than after, the squaring processes then interference terms would appear, giving a much more complicated result. The simple form of $W(\theta)$ stems from the choice of z-axis, since with this choice $m_1 = \pm 1$ only. It would be possible, in principle, to measure the circular polarization of each photon and so, starting from M_i , only one state M is reached, either $M_i + 1$ or $M_i - 1$. Thus there is no interference. However, if an attempt is made to measure linear, rather than circular, polarization of the photons then interference terms appear in $W(\theta)$. Linear polarization can be thought of as a superposition of two oppositely directed circular polarizations and hence there is no sharp value of M but only a probability of $M_i + 1$ or $M_i - 1$. Thus M is no longer a good quantum number and interference terms appear.

2.2 Limitations of the Elementary Theory

The effects of perturbations on the intermediate state are more easily dealt with by means of the density matrix formalism than by modification of the elementary theory. The theory is also restrictive in that $W(\theta)$ depends on the nature of the radiation through the factor $F_\ell^m(\theta)$, which can be derived classically for photons or α particles, but not for β particles. The detectors have

to be polarization insensitive to justify incoherent summing and the special choice of z-axis facilitates the description of one particle, but the second radiation is not simplified.

A more flexible approach is based on the use of the density matrix, described in the next section, and a separate co-ordinate system for each of the radiations. The z-axes of the two co-ordinate systems are chosen to coincide with the directions of emission of the two radiations, and the connection between the radiations is established through the introduction of a third, arbitrary, axis of quantization. The radiation eigenfunctions, quantized with respect to the arbitrary z-axis, are expressed in terms of the eigenfunctions quantized with respect to the directions of emission. These latter eigenfunctions are particularly simple since they correspond to emission with intrinsic angular momentum only, that is to plane waves propagating along the emission direction.

2.3 The Density Matrix Formalism (15,16,17)

In order to appreciate the need for and application of the density matrix formalism, it is helpful to consider the description of states of a single system or an ensemble of systems in both classical and quantum mechanics.

In the case of an individual system the classical description is by a set of canonical co-ordinates and their conjugate momenta. For n degrees of freedom,

the system will be described by $2n$ variables. The quantum mechanical description is by means of a wave function, which is a function of n variables in the case of n degrees of freedom so that the quantum description is more complicated than the classical one.

Now consider an ensemble of systems in the sense of Gibbs, Such an ensemble consists of a very large number of non interacting hypothetical systems introduced to describe one actual system of which our knowledge is only of a statistical nature.

Classically, such an ensemble is represented by a dust of points in a $2n$ dimensional phase space and the dust is described by a density function $\rho(p_r, q_r)$, say. Any single point of the dust, representing one of the hypothetical systems, moves throughout phase space in accordance with Hamilton's equations. The rate of change of ρ , following the motion of the dust, denoted by $\frac{D\rho}{Dt}$, is zero and this constitutes Liouville's Theorem. To obtain the average value of any quantity x over the ensemble, the integral

$$\int x \rho \, dp \, dq$$

must be evaluated over all phase space.

The quantum mechanical description of an ensemble must differ from the classical one since the uncertainty principle denies the possibility of representing each system by a point in phase space. This is where the

density matrix becomes useful for it plays the same part in quantum statistical mechanics as does the distribution function in the classical case. There is a quantum mechanical Liouville Theorem and description of the ensemble is no more complicated than the classical description.

For some physical systems, "maximum" information is not available since the state of the system cannot be specified as completely as is possible without conflicting with the basic principles of quantum mechanics. Such a system, for example an ensemble of radioactive nuclei, cannot be described by a single state, but must be given as an incoherent sum of pure states with appropriate statistical weights.

Let such a system be described by a set of states $|n\rangle$ with statistical weights g_n . The expectation value of any operator F is given by

$$\langle F \rangle = \sum_n g_n \langle n | F | n \rangle .$$

Expand $|n\rangle$ in terms of a complete orthonormal set of basis states $|m\rangle$ by the relations

$$\begin{aligned} |n\rangle &= \sum_m |m\rangle \langle m | n \rangle \\ \text{and } \langle n| &= \sum_{m'} \langle n | m' \rangle \langle m' | \end{aligned}$$

to give

$$\begin{aligned} \langle F \rangle &= \sum_{nmm'} g_n \langle n | m' \rangle \langle m' | F | m \rangle \langle m | n \rangle \\ &= \sum_{nmm'} \langle m' | F | m \rangle \langle m | n \rangle g_n \langle n | m' \rangle . \end{aligned}$$

Then if the density operator ρ is defined by

$$\rho = \sum_n |n\rangle g_n \langle n| ,$$

it follows that

$$\begin{aligned} \langle F \rangle &= \sum_{mm'} \langle m' | F | m \rangle \langle m | \rho | m' \rangle \\ &= \sum_{m'} \langle m' | F \rho | m' \rangle \\ &= \text{Tr}(F\rho) = \text{Tr}(\rho F), \end{aligned}$$

where Tr is the trace, or summation of the diagonal elements, of the matrix $F\rho$ or ρF . There is a double averaging process being performed - statistical, over the ensemble, whereby the weighting factors g_n arise, and the quantum mechanical averaging.

Comparing the classical and quantum cases, it is seen that evaluation of an average is carried out in the former case by integrating over all phase space and in the latter by summing over a complete set of states.

The density matrix is defined by its elements in the particular representation in which the calculation is performed. ρ transforms from one representation to another by means of a unitary transformation but the physically observable $\langle F \rangle$ must obviously be unaffected by the transformation.

The probability of finding any member of a mixed ensemble in the state $|m\rangle$ is given by

$$\sum_n \langle m | n \rangle g_n \langle n | m \rangle = \langle m | \rho | m \rangle .$$

$\text{Tr} \rho$ represents the probability of finding the system

in any one of a complete set of orthonormal states, so that $\text{Tr } \rho = 1$.

2.4 The Density Matrix Description of the Angular Correlation Process.

A nucleus with spin I_i , the initial level being described by a density matrix ρ_i , decays to level I emitting R_1 in direction \underline{k}_1 . This process is described by first order perturbation theory and yields the density matrix $\rho(\underline{k}_1)$. The second step of the cascade is treated in the same manner except that ρ is not known a priori, but depends on the preceding transition. This second step leads to $\rho_f(\underline{k}_1, \underline{k}_2)$ if R_2 is emitted in direction \underline{k}_2 . The probability of finding the nucleus in the final state m_f while the two radiations R_1 and R_2 are observed in directions \underline{k}_1 and \underline{k}_2 is given by

$$\langle m_f | \rho_f(\underline{k}_1, \underline{k}_2) | m_f \rangle$$

and is the required angular correlation function.

Without going into the details of the calculation, which is carried out in full in references (9), (10), (11) and (12), the following points may be noted:-

(a) $\rho(\underline{k}_1, \underline{k}_2)$ may be split up into $\rho(\underline{k}_1) \rho(\underline{k}_2)$. The correlation $w(\underline{k}_1, \underline{k}_2)$ therefore breaks up into two parts, one dependent on each transition.

(b) The calculation reduces essentially to the evaluation of matrix elements of the type

$$\langle I M \underline{k} \sigma | H | I_i M_i \rangle = \langle f | H | i \rangle$$

where $|i\rangle$ is a state vector for a nucleus with spin I_1 and z component M_1 , $\langle f|$ describes the final nuclear state I, M and the radiation in direction \underline{k} with spin σ , and H is the operator of the interaction which causes the transition.

Such a matrix element may be broken down into a product of a phase factor, a Clebsch-Gordan coefficient, a plane wave eigenfunction, a reduced matrix element and a rotation matrix. The rotation matrix comes in through the transformation which expresses the radiation eigenfunctions in an arbitrary co-ordinate system in terms of the simpler plane wave eigenfunctions which are referred to a co-ordinate system having the propagation direction as z -axis.

(c) The final expression for W is a product of four such matrix elements and is accordingly very complex, but it contains factors which depend on the properties of the radiation only. When these factors are singled out, they are said to constitute the radiation parameters. The remainder of the expression then contains Clebsch-Gordan coefficients, reduced matrix elements and a rotation matrix,

(d) The angular correlation function $W(\theta)$ reduces to a simple form when directions, but not polarizations, are observed, for then the rotation matrix elements reduce to Legendre Polynomials $P_k(\cos \theta)$, where k is even and subject to the selection rules

$$0 < k < \text{Min}(2I, 2l_1, 2l_2)$$

$$0 < k < \text{Min}(2I, l_1 + l_1', l_2 + l_2')$$

for pure and mixed multipoles respectively.

Then $W(\theta)$ is expressed as

$$W(\theta) = \sum_{k=0}^{k_{\max}} A_{kk} P_k(\cos \theta)$$

where A_{kk} breaks up into two factors, one for each transition. For pure multipoles l_1 and l_2 ,

$$A_{kk} = F_k(l_1 l_1 I_i I) F_k(l_2 l_2 I_f I)$$

where the F_k are tabulated numbers⁽¹¹⁾.

For mixed transitions in the scheme

$$I_i \xrightarrow{l_1+l_1'} I \xrightarrow{l_2+l_2'} I_f,$$

$$A_{kk} = A_k(l_1 l_1' I_i I) A_k(l_2 l_2' I_f I) \quad \text{must be}$$

calculated in terms of the amplitude mixing ratio $\partial(\gamma)$ by the formula

$$A_k(l_1 l_1' I_i I) = \frac{F_k(l_1 l_1 I_i I) + 2\partial_1 F_k(l_1 l_1' I_i I) + \partial_1^2 F_k(l_1' l_1' I_i I)}{(1 + \partial_1^2)}$$

with a similar expression for $A_k(l_2 l_2' I_f I)$.

$\partial_1(\gamma)$ is the ratio of reduced matrix elements

$$\frac{\langle I || l_1' \pi_1' || I_i \rangle}{\langle I || l_1 \pi_1 || I_i \rangle}$$

(e) In the general formula for $W(\theta)$ the factors which depend on the type of radiation are the radiation parameters and the reduced matrix elements. Radiation parameters can be calculated for any radiation and reduced matrix elements are not important since they only enter the correlation when there is multipole mixture and even then only as ratios of l and l' components through the factor δ defined above. Hence, in theory, any angular correlation involving arbitrary radiations can be calculated. In practice, it is found convenient to adopt the γ - γ angular correlation as a standard and to express the correlations for any other radiation in terms of this standard. Particle parameters, denoted by $b_k(l l'; x)$ are therefore defined for radiation x as the ratio of the x radiation parameter to the γ radiation parameter. Reduced matrix elements occurring for γ emission must be replaced by those appropriate to the radiation x .

Hence for arbitrary radiations R_1 and R_2 ,

$$W_{R_1 R_2}(\theta) = \sum_{k=0}^{k_{\max}} A_{kk} P_k(\cos \theta)$$

where $A_{kk} = b_k(l_1 l_1'; R_1) F_k(l_1 l_1' I_1 I_1) b_k(l_2 l_2'; R_2) F_k(l_2 l_2' I_2 I_2)$.

The result is easily generalized to include multipole mixtures.

(f) The density matrix method is capable of taking the effect of extra nuclear fields into account simply by allowing the density matrix of the intermediate state to vary in time. The change, if any, in ρ takes place during the time the intermediate state is exposed to the extra nuclear field and can be expressed by a unitary transformation whose form depends on the nature of the extra nuclear interaction. Perturbation of the intermediate state can occur by interaction of the nuclear magnetic moment with the magnetic field of the electronic shells or by interaction of the nuclear electric quadrupole moment with inhomogeneous electric fields.

2.5 The Theory of β Decay

(a) Introduction

β decay is the process whereby electrons having a continuous energy spectrum are emitted from radioactive nuclei. The necessity of explaining the continuous spectrum led to the neutrino hypothesis of Pauli and a theory of the process, incorporating the neutrino, was first given by Fermi⁽¹⁸⁾. The Fermi theory of β decay, generalized and slightly modified in the light of experimental results, is the currently accepted description of the process.

Fermi's theory was constructed in analogy to the theory of emission of a photon from an excited atom. The electron and anti-neutrino are pictured as being created

when a neutron transforms into a proton. The mathematical formalism appropriate to the description of such a process is that of second quantization, where the probability amplitudes ψ , ϕ for electrons and neutrinos are viewed as operators. This description is appropriate because the total number of electrons and neutrinos is not constant.

(b) The β decay Interaction

The energy of the complete system consisting of heavy and light particles is a sum of three terms, one for the heavy particles (nucleons), one for the light particles (leptons) and the interaction energy, H_β , between nucleons and leptons. The term H_β is regarded as a perturbation energy and, once its form has been decided, the methods of time dependent perturbation theory are available to calculate the transition probability of the process. The β decay probability of a nucleus is proportional to the square of the matrix element

$$M_\beta = \langle \Psi_f \psi \phi | H_\beta | \Psi_i \rangle \quad (1)$$

where Ψ_i , Ψ_f refer to the initial and final nuclear states, ψ and ϕ refer to electron and neutrino states.

The theory by which the energy spectrum is calculated requires evaluation of expressions of the type

$$\left| \sum_k \int M_\beta \delta(\underline{E} - \underline{E}_k) dV_k \right|^2 \quad (2)$$

The summation is over all nucleons (co-ordinates \underline{E}_k) and

the integration is over the nuclear volume. The factor $\delta(\underline{r} - \underline{r}_k)$ states that the interaction is taken to be local. In addition, a sum over all unobserved quantities has to be performed. These will include the angular momentum quantum numbers or spin directions of leptons, magnetic sub-states of nuclear levels and, except in angular correlations, the directions of motion of the leptons.

In order to formulate H_β , appeal must be made to the conservation laws. Momentum and angular momentum must be conserved and invariance under Lorentz transformations ensured. Such considerations alone are not sufficient to specify unambiguously the form of H_β and it can be shown that the most general interaction consistent with the relativistic requirements is a sum of five terms

$$H_\beta = C_S H_S + C_V H_V + C_T H_T + C_A H_A + C_P H_P$$

where the C_i 's are constants and

$$\left. \begin{aligned} H_S &= g(\Psi_f^* \beta \Psi_i)(\psi^* \beta \phi) \\ H_V &= g[(\Psi_f^* \Psi_i)(\psi^* \phi) - (\Psi_f^* \underline{\alpha} \Psi_i)(\psi^* \underline{\alpha} \phi)] \\ H_T &= g[(\Psi_f^* \beta \underline{\sigma} \Psi_i)(\psi^* \beta \underline{\sigma} \phi) + (\Psi_f^* \beta \underline{\alpha} \Psi_i)(\psi^* \beta \underline{\alpha} \phi)] \\ H_A &= g[(\Psi_f^* \underline{\sigma} \Psi_i)(\psi^* \underline{\sigma} \phi) - (\Psi_f^* \underline{\gamma}_5 \Psi_i)(\psi^* \underline{\gamma}_5 \phi)] \\ H_P &= g(\Psi_f^* \beta \underline{\gamma}_5 \Psi_i)(\psi^* \beta \underline{\gamma}_5 \phi) \end{aligned} \right\} (3)$$

The suffixes S,V,T,A,P indicate that the terms are scalar contractions of two scalars, vectors, tensors of second rank, axial vectors or pseudo scalars. g is a

constant expressing the strength of the interaction. \underline{a} , β are the Dirac matrices as defined, for example, by Konopinski and Uhlenbeck⁽¹⁹⁾.

$$\gamma_5 = \gamma_1 \gamma_2 \gamma_3 \gamma_4 \quad \text{where}$$

$$\gamma_k = -i \alpha_k \beta \quad \text{for } k = 1, 2, 3.$$

and $\gamma_4 = \beta$.

Also $\underline{\sigma} = \gamma_5 \underline{a}$.

Formally, it is necessary to insert an operator into the expressions (3) which transforms a neutron into a proton. Also, the Hermitian conjugate of each term should be added to allow for positron emission.

(c) Recent Developments of the Theory

The proposal of Lee and Yang⁽²⁰⁾ that parity might not be conserved in weak interactions and the verification of this idea by Wu et al.⁽²¹⁾, have made it necessary that H_β be a linear combination of scalar and pseudo-scalar terms. H_β should therefore be written as

$$H_\beta = \sum_{i=1}^5 C_i H_i + \sum_{i=1}^5 C_i' H_i'$$

where the Hamiltonian now has a parity conserving and a parity non-conserving part.

Analysis of experimental results (see, for example, Konopinski⁽²²⁾) has led to the conclusion that, of the five possible interactions, only the V and A terms

need be incorporated in H_β . These interactions enter with opposite phases so that the total interaction is usually referred to as the "V-A" interaction.

Experimental evidence (e.g. electron polarization) shows that fermions appear to participate in the β interaction only through the left-handed components of their states (and through right-handed components of anti-particle states). The formal description of such components is by means of the operator γ_5 . The left-handed projection of a state Ψ is Φ , say, given by

$$\Phi = \frac{1}{2}(1 + \gamma_5) \Psi.$$

A more general and fundamental picture of the β decay process regards it as the result of an interaction between two four-vector currents, each containing a vector and an axial vector part. One current contains annihilation and creation operators for strongly interacting particles and the other contains such operators for leptons.

The review article of Blin-Stoyle and Nair⁽²³⁾ shows how an interaction between these currents of the form $\mathcal{H}_\beta \sim J_\alpha(pn)J_\alpha(ev)$ leads to the familiar theory of β decay.

Using left-handed projections, the nucleonic current can be written as

$$J_\alpha(pn) = \bar{\Psi}^* \frac{1}{2}(1 + \gamma_5) \beta \gamma_\alpha \tau_+ \Psi$$

where τ_+ is the operator which transforms a neutron into a proton. H_β then takes the form

$$H_\beta = 2^{1/2} g(1 + \gamma_5) \beta \gamma_\alpha \tau_+ J_\alpha(e\nu) + \text{Hermitian conjugate} .$$

[Since $h_\beta \equiv \langle \bar{\Psi} | H_\beta | \Psi \rangle$].

For an entire nucleus

$$H_\beta(A) = 8^{1/2} g \sum_{a=1}^A \frac{1}{2}(1 + \gamma_5^a) \beta^a \gamma_\alpha^a \tau_+^a [J_\alpha(e\nu)]_{\underline{r}_a} + \text{H.C.}$$

where the lepton current is evaluated at the position of the transforming nucleon. The nucleon current can be split into vector and axial vector parts. Assuming that the coupling constants associated with the V and A couplings are not equal and remembering that the law is V-A, the generalized coupling form is

$$H_\beta = 2^{1/2} g \sum_{a=1}^A (C_V - C_A \gamma_5^a) \beta^a \gamma_\alpha^a \tau_+^a [J_\alpha(e\nu)]_{\underline{r}_a} + \text{H.C.}$$

The lepton current $J_\alpha(e\nu)$ is

$$J_\alpha = \bar{\psi} \gamma_\alpha (1 + \gamma_5) \psi$$

where $\bar{\psi} = \psi^* \beta = \psi^* \gamma_4$.

Having discussed these formal aspects of the theory it is now possible to demonstrate the various approximations used in the calculation of transition probabilities.

(d) The Allowed Transitions

The expressions H_V and H_A contain terms of order v/c where v is the nucleon speed, namely the terms containing $\underline{\alpha}$ and γ_5 . Ignoring these gives

$$H_V = g(\bar{\Psi}_f \Psi_i)(\psi^* \beta)$$

$$H_A = g(\bar{\Psi}_f \underline{\alpha} \Psi_i)(\psi^* \underline{\alpha} \beta),$$

and H_V and H_A have to be used in the evaluation (1) of section (b).

Ignoring the, presumably slight, variations in lepton wave functions across the nuclear volume, the lepton terms can be taken outside the integration sign in equation (2) of section (b). If it is further assumed that the lepton wave functions may be taken to be plane waves of the form $\exp i \underline{p} \cdot \underline{r}$, $\exp i \underline{q} \cdot \underline{r}$ for electron and neutrino respectively, then the function $\exp i(\underline{p} + \underline{q}) \cdot \underline{r}$ may be expanded as a power series in \underline{r} and the first term only retained. This constitutes the allowed approximation. The nuclear matrix elements remaining are

$$\int \Psi_f^* \Psi_i \, dV \quad \text{and} \quad \int \Psi_f^* \underline{\sigma} \Psi_i \, dV$$

and are conventionally abbreviated to $\int \mathbf{1}$ and $\int \underline{\sigma}$ respectively.

Nuclear states have definite spin and parity values and therefore the matrix elements $\int \mathbf{1}$ and $\int \underline{\sigma}$ determine the allowed selection rules, namely

$$\Delta J = 0, \quad \Delta \pi = \text{no}, \quad \text{from } \int \mathbf{1}$$

$$\Delta J = \pm 1, 0 \quad (\text{no } 0 \rightarrow 0), \quad \Delta \pi = \text{no}, \quad \text{from } \int \underline{\sigma}.$$

These are known as the Fermi and Gamow-Teller selection rules. The Fermi rule arises from the V interaction (the one considered by Fermi in his fundamental paper⁽¹⁸⁾) and the Gamow-Teller rule from the A interaction.

(e) The Forbidden Transitions

If the spins and parities of two nuclear states are such that the allowed selection rules cannot be complied with, this does not necessarily mean that β decay between the two states cannot take place, but rather that the approximations used in deriving the allowed selection rules must be re-considered.

The approximations used were of two types:

- (i) neglect of relativistic terms of order v/c
- (ii) neglect of higher than first order terms in the expansion $\exp. i(\underline{p} + \underline{q}) \cdot \underline{r}$.

Retaining the relativistic term in the V interaction gives a nuclear matrix element $\int \underline{a}$, in the previous notation. Keeping the first power of \underline{r} in the series expansion gives $\int \underline{r}$. $\int \underline{a}$ and $\int \underline{r}$ are expected to be of the same order of magnitude (19).

The selection rules are :

$$\begin{aligned} \int \underline{a} & : \Delta J = 0, \pm 1 \quad (\text{no } 0 \rightarrow 0), \quad \Delta \pi = \text{yes} \\ \int \underline{r} & : \Delta J = 0, \pm 1 \quad (\text{no } 0 \rightarrow 0), \quad \Delta \pi = \text{yes.} \end{aligned}$$

Similarly in the next highest approximation, the A interaction yields matrix elements

$$\int \gamma_5, \quad \int \underline{\sigma} \cdot \underline{r}, \quad \int \underline{\sigma} \times \underline{r}, \quad \int B_{ij} = \int [\sigma_i x_j + \sigma_j x_i - \frac{2}{3} \delta_{ij} (\underline{\sigma} \cdot \underline{r})]$$

with selection rules:

$$\begin{aligned} \int \gamma_5 & : \Delta J = 0, \quad \Delta \pi = \text{yes} \\ \int \underline{\sigma} \cdot \underline{r} & : \Delta J = 0, \quad \Delta \pi = \text{yes.} \end{aligned}$$

$$\int \underline{\sigma} \times \underline{r} : \Delta J = 0, \pm 1 \text{ (no } 0 \rightarrow 0), \Delta \pi = \text{yes}$$

$$\int B_{ij} : \Delta J = 0, \pm 1, \pm 2 \text{ (no } 0 \rightarrow 0, \frac{1}{2} \rightarrow \frac{1}{2}, 1 \rightarrow 0),$$

$$\Delta \pi = \text{yes.}$$

$\underline{\sigma} \cdot \underline{r}$, $\underline{\sigma} \times \underline{r}$ and B_{ij} are the irreducible components of the general product of $\underline{\sigma}$ and \underline{r} .

This retention of the next highest order of terms gives the selection rules for first forbidden decay. The fact that there are six matrix elements contributing to first forbidden decay makes their experimental determination a difficult procedure.

Taking further terms in the expansion of $\exp. i(\underline{p} + \underline{q}) \cdot \underline{r}$ leads to selection rules for still higher degrees of forbiddenness. In general, the n-th forbidden group occurs through matrix elements of the (n+1)-th term of the power series expansion combined with the operator 1 and $\underline{\sigma}$ (for V and A respectively) and of the n-th term of the power series expansion combined with the velocity dependent operators \underline{q} and γ_5 (for V and A respectively).

(f) Coulomb Corrections: The "Normal" and "g" Approximations

The assumption of plane wave eigenfunctions is justified for the neutrino, but the appropriate wave functions for the electron are the solutions of the Dirac equation for an electron in the Coulomb potential set up by the nucleus. Even here it is customary to introduce simplifying assumptions. Thus, as a first approximation, the potential may be taken as that of a point charge, but

the effects of finite nuclear size and screening by atomic electrons should be taken into account. The selection rules already deduced for the various degrees of forbiddenness will not be altered by this more refined procedure.

The lepton functions are now taken to be bilinear combinations of radial functions (solutions of the Dirac equation for an electron in a Coulomb field and for a free neutrino), and if only the lowest contributing powers of ξ are kept, then this is called the normal approximation. The normal approximation is expected to hold for small Z (≤ 10). For large Z (≥ 20) the magnitude of the lepton terms is determined by the term with the highest power of the parameter $\xi = \frac{\alpha Z}{2R}$, corresponding to half the electron potential energy at the nuclear surface. (Units used in β decay theory are such that $\hbar = m = c = 1$, where m is the electronic rest mass. In these units the electronic charge is $(\alpha)^{1/2} = (137)^{-1/2}$, where α is the "fine structure constant." The radius of a nucleus is approximately $2^{2/5} \alpha A^{1/3}$). This means that the presence of the nuclear Coulomb field distorts the wave functions to such an extent that terms arise which are more significant than the next lowest terms in the field free (plane wave) expansion. If $\xi \gg W_0 - 1$, where W_0 is the maximum electron energy, then only the terms with the highest power of ξ need be retained. This forms the basis of the ξ , or Coulomb, approximation.

The matrix element B_{ij} does not contribute to the

ξ approximation in first forbidden β decay, but is the only matrix element contributing to the "unique" first forbidden decay where $\Delta J = 2$, $\Delta\pi = \text{yes}$. (Wiedenmüller⁽²⁴⁾),

(g) The Energy Spectrum and log ft Values

The result of the time dependent perturbation theory calculation is that the electron energy distribution is given by

$$P(W)dW = \frac{g^2}{2\pi^3} F(Z,W)pW(W_0-W)^2 S_n(W,Z)dW .$$

Here, $F(Z,W)$ is the Fermi function representing the influence of the nuclear charge Z . It is essentially the ratio of the electron density at the nucleus to that at infinity. Thus $F = 1$ for $Z = 0$. p, W are the electron momentum and energy respectively and W_0 is the maximum energy of the β spectrum. The factor $pW(W_0-W)^2$ represents the statistical sharing of energy between electron and neutrino. $S_n(W,Z)$ is the shape correction factor for an n -th forbidden transition. It contains the nuclear matrix elements and the radial lepton functions. For allowed transitions, $S_0(W,Z)$ is independent of lepton energy and the resulting spectrum is said to have "statistical" shape since the energy dependence is contained wholly in the factor $pW(W_0-W)^2$, apart from the Coulomb distortion given by $F(Z,W)$.

Conformity to statistical shape is checked by drawing the "Kurie plot", where the quantity $\left[\frac{N(W)}{pWF} \right]^{1/2}$ is calculated (N is the experimentally observed number of

electrons per unit energy interval) and plotted against W . Such a plot should yield a straight line for a statistical spectrum. The additional dependence on electron energy introduced through the shape factor S_n leads to the expectation of non-linear Kurie plots for forbidden spectra. In ξ approximation, however, the shape factor is independent of lepton energy and therefore first forbidden spectra might be expected to exhibit an allowed shape. This has been confirmed experimentally for many first forbidden transitions.

The total decay rate from one nuclear state to another is obtained by integrating the energy spectrum. Thus the disintegration constant, λ , is given by

$$\lambda = \int_1^{W_0} P(W) dW = \frac{g^2}{2\pi^3} \int_1^{W_0} F(Z, W) pW(W_0 - W)^2 S_n(Z, W) dW.$$

The half life, t , is related to λ by

$$t = \log_e 2 / \lambda$$

and, for an allowed transition, since $S_0(Z, W) = C_V^2 [\int 1]^2 + C_A^2 [\int \underline{g}]^2$ is energy independent,

$$ft = \log_e 2 \frac{2\pi^3}{g^2} \cdot \frac{1}{C_V^2 (\int 1)^2 + C_A^2 (\int \underline{g})^2},$$

where f is the tabulated function

$$\int_1^{W_0} F(Z, W) pW(W_0 - W)^2 dW.$$

The half life is not in itself characteristic of an

allowed decay since it is strongly energy dependent ($t \sim W_0^{-5}$) but the product ft should be fairly uniform within any appropriately chosen family of nuclei, that is in cases where the nuclear matrix elements are expected to be of comparable size. The formation of the product ft using experimentally observed half lives and calculated values of f may be regarded as a means of eliminating the effect of the special energy release and charge associated with a particular decay.

The situation is more complicated in the case of forbidden decays because, in general, S_n is energy dependent. However the matrix elements decrease by approximately a factor of ten from one degree of forbiddenness to the next higher one and it might therefore be expected that ft values derived experimentally should fall into well defined groups, each group corresponding to a definite degree of forbiddenness. Since values of ft vary over a wide range, it is customary to quote the $\log_{10}ft$ value of a decay, t being measured in seconds.

It is found that, with some exceptions, notably in the regions of deformed nuclei and of high Z (~ 80), $\log_{10}ft$ values fall within the following ranges:

3 - 3.7 and 4 - 6	-	allowed
6 - 8	-	first forbidden
8 - 10	-	first forbidden unique
12 - 14	-	second forbidden

18	-	third forbidden
23	-	fourth forbidden (single case).

(h) The $\beta - \gamma$ Angular Correlation

The form of the correlation function is

$$W(\theta) = \sum_k A_k(\beta) A_k(\gamma) P_k(\cos \theta)$$

$$\text{where } A_k(\beta) = \sum_{JJ'} \frac{F_J(JJ'I_i I) b_k(JJ')}{\sum_J b_0(J,J)}$$

and the b_k are β particle parameters as defined in reference (11). These β parameters actually include the reduced nuclear matrix elements. J refers to the total angular momentum carried away by the electron-neutrino pair.

The theory of $\beta - \gamma$ angular correlations yields the following results⁽¹¹⁾:

In the case of allowed decays, the $\beta - \gamma$ correlation is isotropic. There might be a very small anisotropy, but this can only occur under very special circumstances, that is when the allowed matrix elements are somehow greatly inhibited and second forbidden matrix elements with amplitudes down by a factor of one hundred might then contribute. In such a case there would of course be no possibility of a contribution from the larger (i.e. down by a factor of ten) first forbidden matrix elements since these would be prohibited completely by the parity selection rule.

For first forbidden decays, the correlation has the form

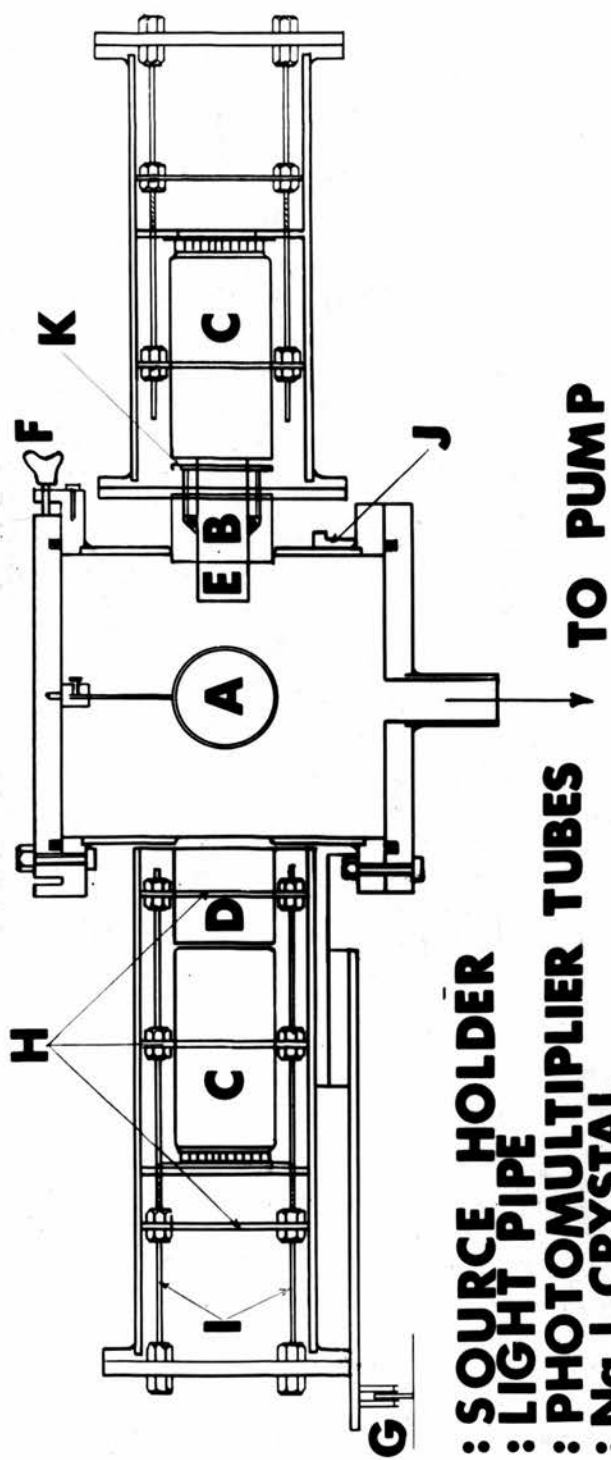
$$W(\theta) = 1 + A_2(\beta) A_2(\gamma) P_2(\cos \theta) .$$

Evaluation of $A_2(\beta)$ requires knowledge of the b_2 β parameters, which in turn involve lepton wave functions and nuclear matrix elements. If the ξ approximation holds exactly, that is if only the highest powered term in ξ in the wave function expansion exists, then the correlation is isotropic. However, taking into account all the next lowest term in ξ yields $A_2(\beta) \sim \frac{1}{\epsilon^2}$. Thus the second term in the expansion contains the first non-zero contributing term to $W(\theta)$. $A_2(\beta)$ is energy dependent, the dependence being as p^2/W .

First forbidden transitions may therefore be expected to show a small anisotropy in the $\beta - \gamma$ angular correlation, the size of the anisotropy and its energy dependence providing a check as to the validity of the ξ approximation to the decay in question. If the decay is well described in ξ approximation, it is very difficult to determine individual nuclear matrix elements since the expression for $A_2(\beta)$ involves only ratios of certain linear combinations of nuclear matrix elements (11).

β transitions which deviate from the ξ approximation have proved of particular interest and value because in such cases it is possible to measure the individual matrix elements. Deviations may arise as a result of accidental cancellation of otherwise large

matrix elements or because of some selection rule which, in the case of first forbidden decay, causes the tensor type nuclear matrix element $\int B_{ij}$ (ignored in ξ approximation) to be enhanced relative to the other matrix elements. Such a decay will normally have a high $\log ft$ value, a non-statistical spectrum shape and a large $A_2(\beta)$ coefficient, as is the case in the β decay of ${}_{84}^{152}\text{En}$.



- A : SOURCE HOLDER**
- B : LIGHT PIPE**
- C : PHOTOMULTIPLIER TUBES**
- D : Na I CRYSTAL**
- E : PLASTIC SCINTILLATOR**
- F : ADJUSTING SCREW**
- G : TROLLEY**
- H : POSITIONING RINGS**
- I : SCREWED RODS**
- J : COLLAR**
- K : LIGHT PIPE HOLDER**

FIGURE 4 (a.)

CHAPTER 3

3.1 The Angular Correlation Chamber

The angular correlation chamber, shown in Figure 4(a), was made from a brass cylinder 6" high, 6" in diameter and of $\frac{1}{8}$ " wall thickness. The central 2" portion of wall was turned down to $\frac{1}{16}$ " thickness in order to minimize γ ray absorption, particularly that of the weak 729 keV γ ray of ThC'. Using the absorption coefficient tables of Davisson and Evans⁽²⁵⁾, it was estimated that there would be an intensity reduction of approximately 7% in a γ ray, of this energy, passing through $\frac{1}{16}$ " brass. Absorption of the other γ rays of interest was not important because of their much higher intensities. Provision was made for evacuation of the chamber through a brass tube set into the base carrying a Pirani vacuum gauge head and a needle valve. Using a backing pump, pressures of 10^{-3} mm. of mercury were achieved and an elementary approximate calculation shows that the electron mean free path at such a pressure is much greater than the chamber diameter. A close fitting brass collar surrounded the chamber and the γ detector was mounted in a grooved block of wood on a trolley attached to the collar. A flange set into the chamber wall carried the β detector and a perspex light guide.

3.2 The Source Holder

The source holder consisted of two 2" diameter aluminium rings clamped together and mounted on a brass rod. Aluminium foils, on which the sources were deposited, could then be inserted between the rings and held in position by means of three 10 B.A. nuts and bolts.

The source holder was suspended from the centre of the chamber lid which could be moved by screws fixed to the top flange of the chamber (see Figure 4(a)), thus allowing the sources to be centred.

3.3 The β and γ Detectors

The β detector was a cylindrical piece of "NE 102A" plastic scintillator, $\frac{27}{32}$ " in diameter and $\frac{2}{5}$ " high. Such a thickness of plastic is just sufficient to stop the most energetic β particles emitted from a source of the thorium active deposit. The plastic was coated on the sides with a reflecting paint and the front face was covered with 100 $\mu\text{gm} / \text{cm}^2$ aluminium foil. Optical contact of plastic to light pipe and light pipe to photomultiplier tube was obtained using "Midland-Silicone" jelly, a material which was found to give excellent coupling. The photomultiplier, E.M.I. type 6097B and dynode resistor chain were mounted inside a brass tube having a flange at each end so that the tube could be bolted to the flange set into the chamber wall while a cathode follower was screwed to the far end.

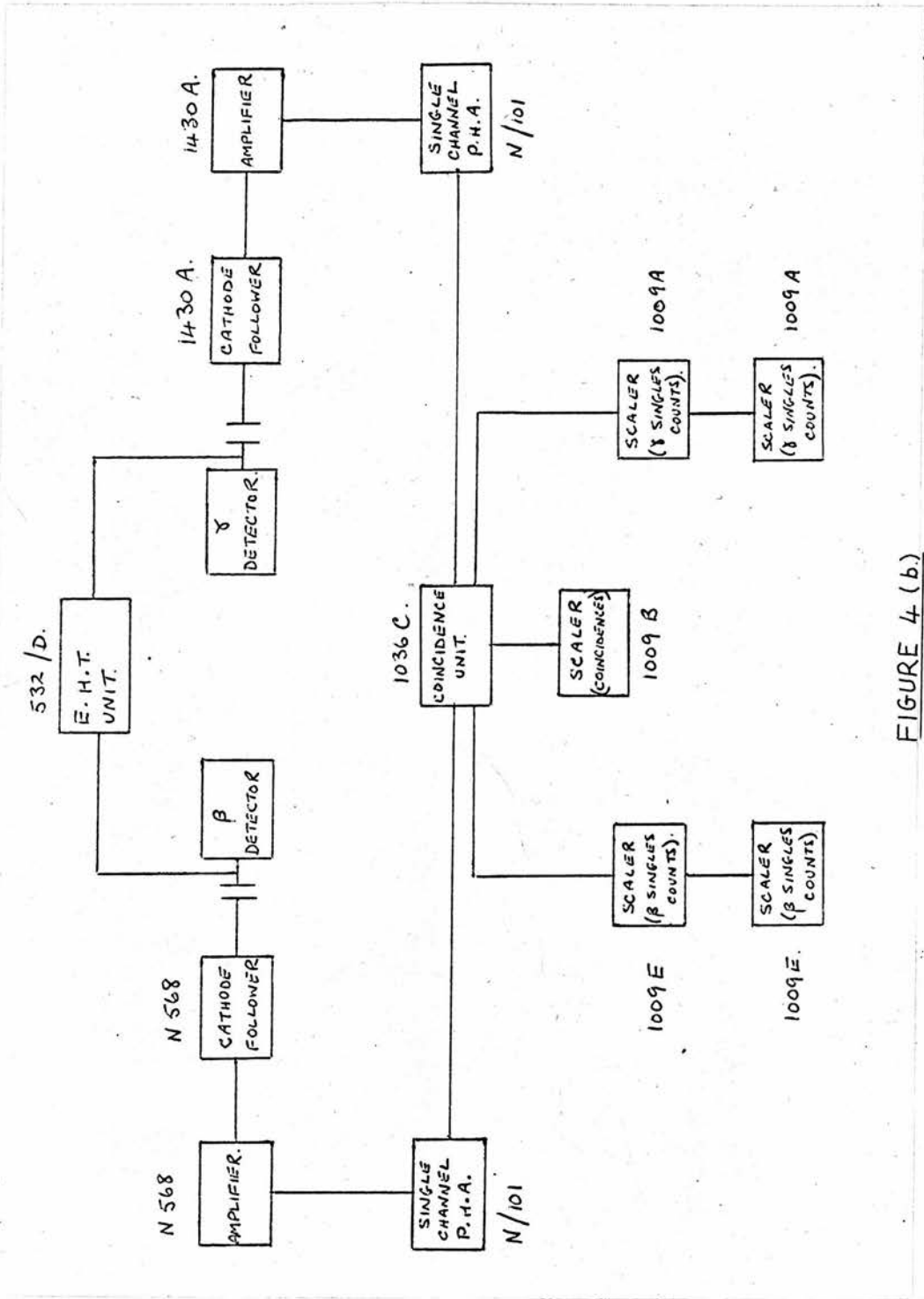


FIGURE 4 (b.)

The γ detector was a 2" x 2" sodium iodide crystal optically coupled to a type 6097B photomultiplier using the "Midland-Silicone" jelly. Crystal, photomultiplier and dynode chain were mounted inside a paxolin tube with a $\frac{25}{1000}$ " aluminium disc press-fitted into one end. The other end of the paxolin tube was flanged, and carried a cathode follower.

3.4 The Electronics

The electronics used in this work was of standard type. In each case, negative pulses were taken from the anode of the photomultiplier and fed through a cathode follower, amplifier and single channel pulse height analyser to a coincidence unit and scalers. In order to record the single channel counts, it was necessary to use two scalers in series for each of the two channels. The photomultiplier tubes were run at 1400 volts, supplied by an "Isotope Developments" E.H.T. unit, type 532/D. The integration and differentiation time constants on the amplifiers were adjusted until the pulses in each case were positive, of approximately 2 μ sec. duration and had as small a negative overshoot as possible. Figure 4(b) shows a block diagram of the electronic system.

3.5 β and γ Spectra

Figures 5 - 9 show some typical β and γ spectra measured using the detectors and electronics described

↑
[COUNTS PER 30 SECONDS] × 10⁻³

FIGURE 5.

LOW ENERGY γ SPECTRUM
OF E_{μ}^{152}

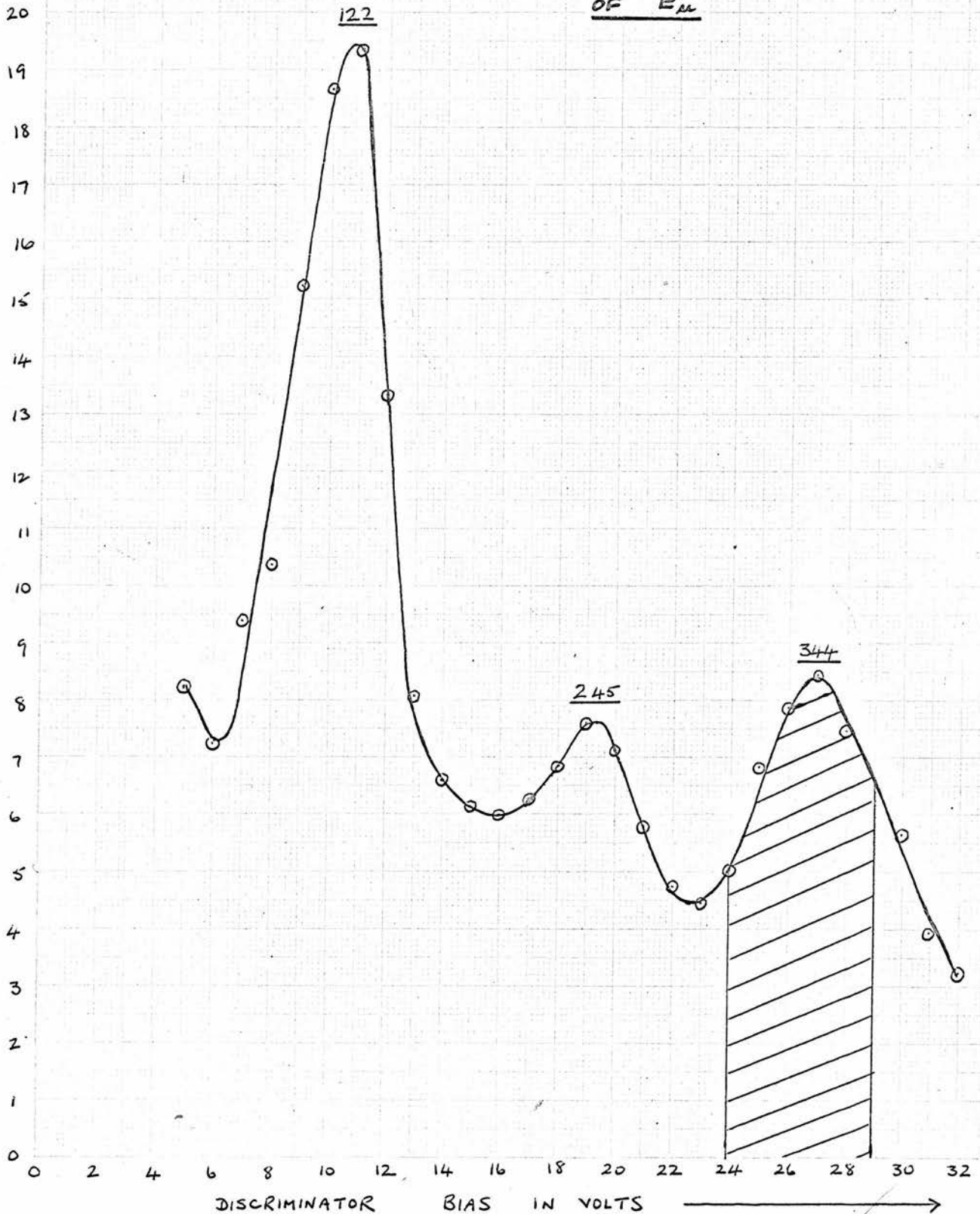
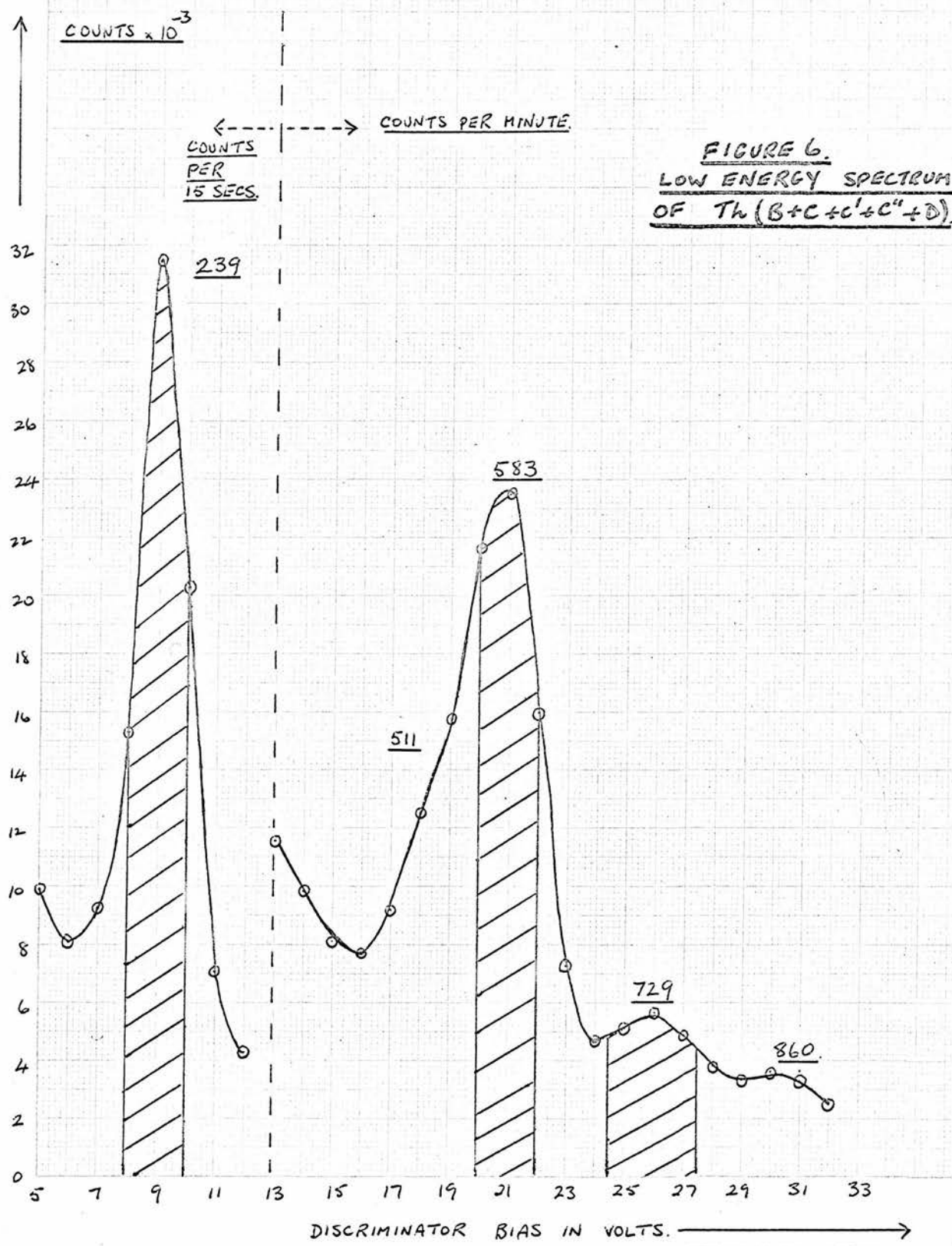


FIGURE 6.
LOW ENERGY SPECTRUM
OF Th (B+C+C'+C''+D).



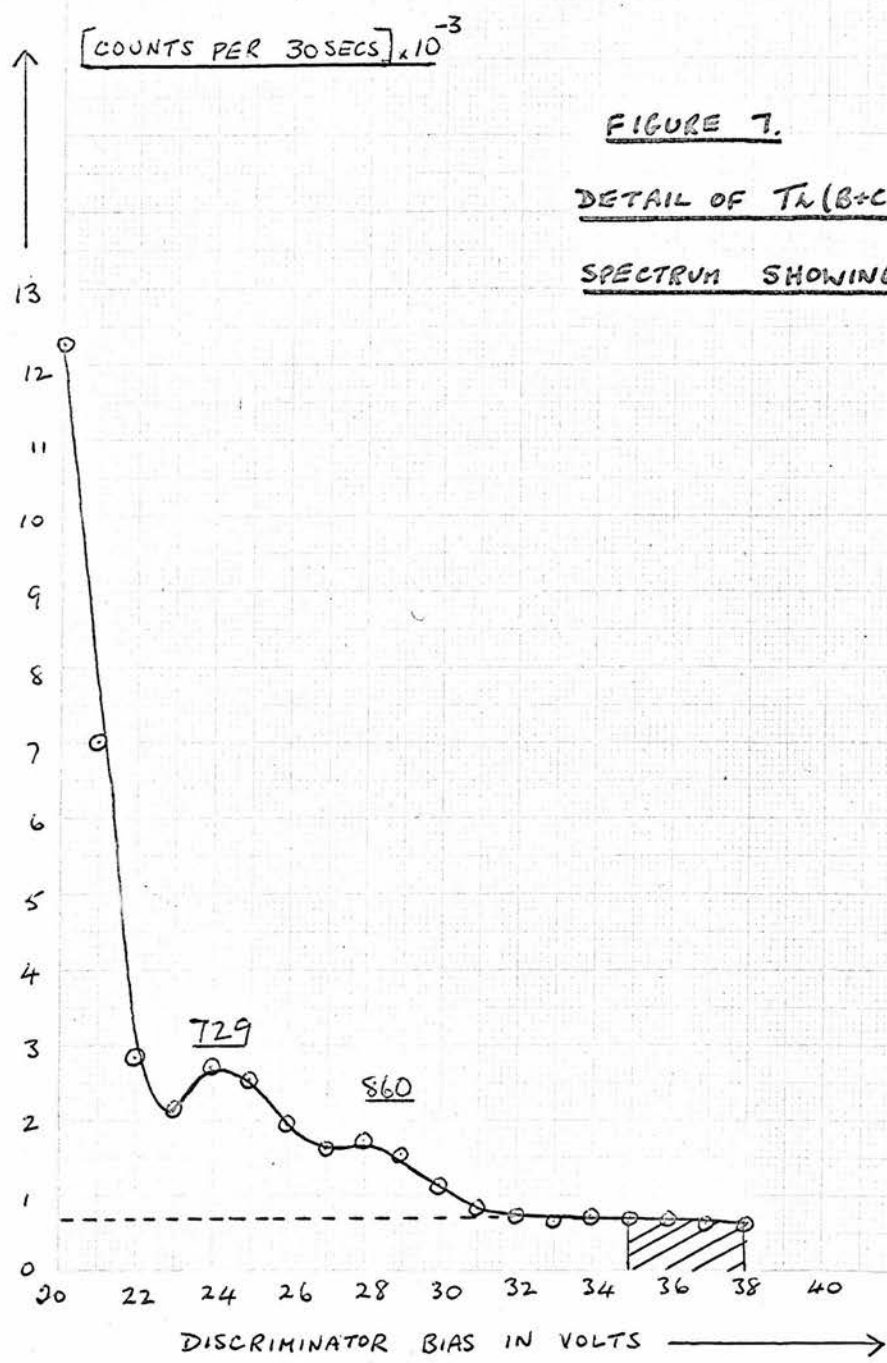


FIGURE 8.
HIGH ENERGY SPECTRUM
OF $T\alpha(B+C+C'+C''+D)$.

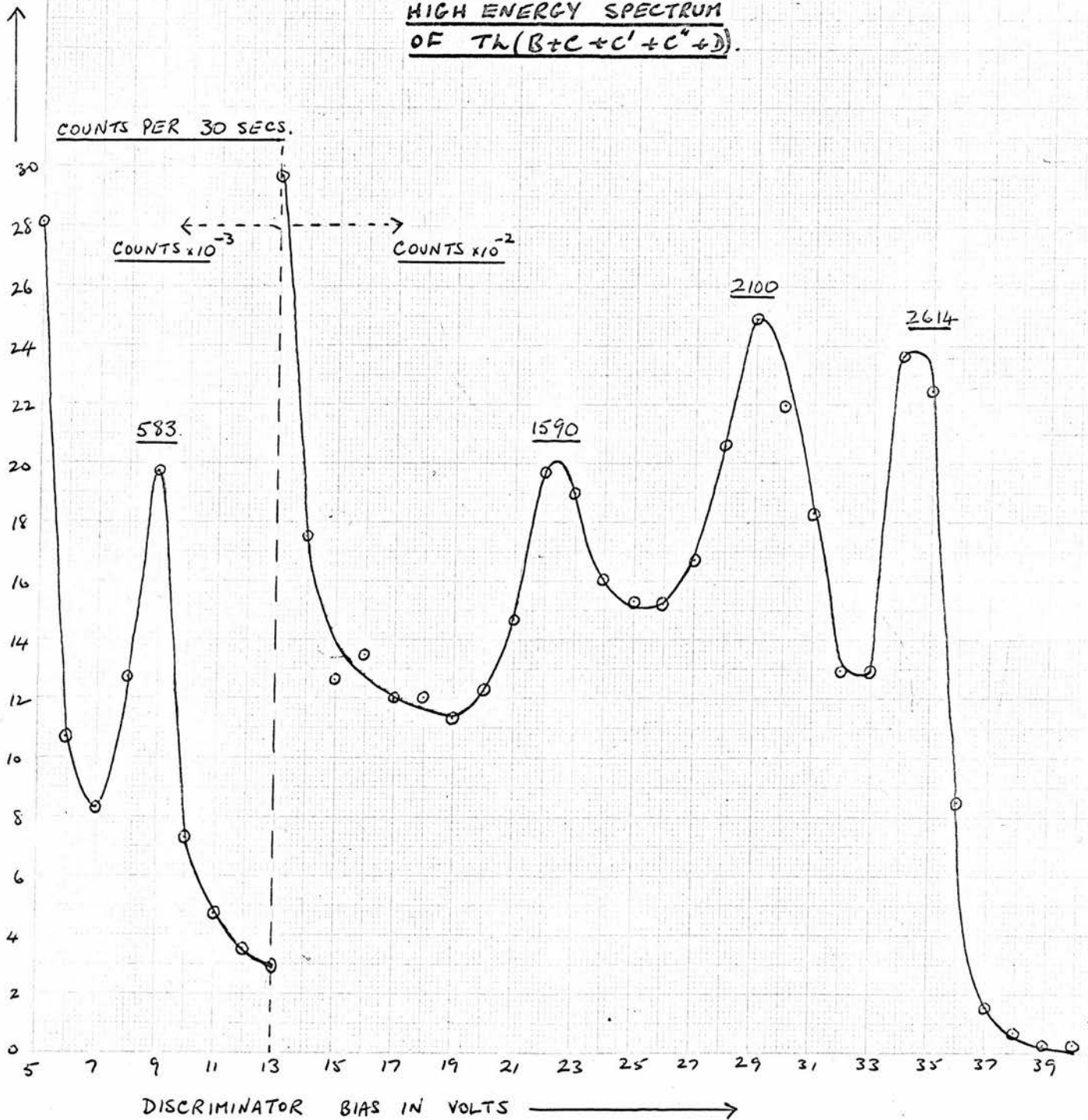
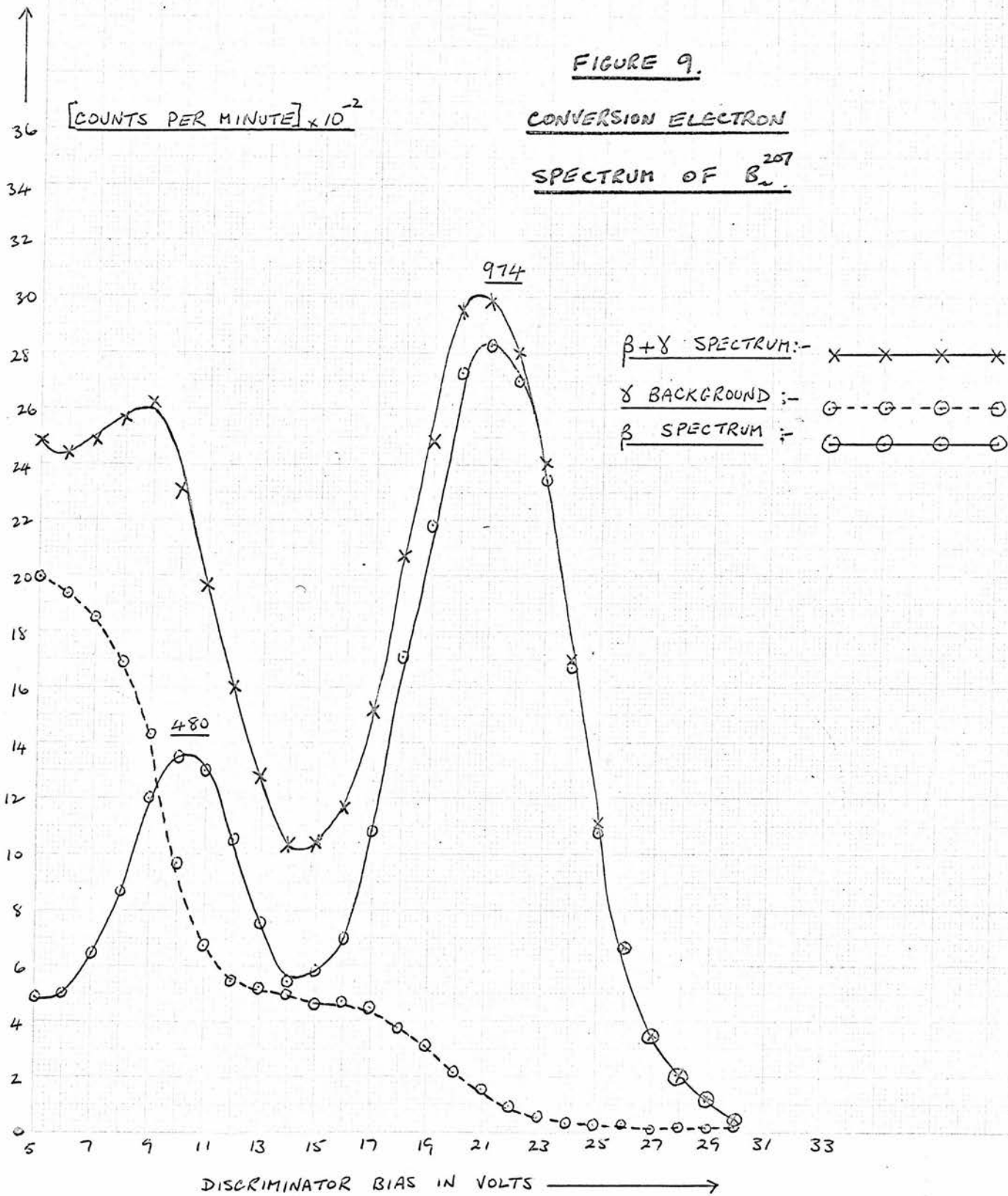


FIGURE 9.

CONVERSION ELECTRON

SPECTRUM OF B_{207}



above, with a 1 v. channel width in the single channel pulse height analysers. Figure 5 shows the low energy γ spectrum of ${}_{82}^{152}\text{Eu}$ with the line at 344 keV, used in the angular correlation experiment, standing out clearly. The lines at 122 and 245 keV belong to ${}_{90}^{152}\text{Sm}$ which is reached from ${}_{89}^{152}\text{Eu}$ by means of β^+ emission and electron capture. Figures 6, 7 and 8 show various details of the γ spectrum of the thorium active deposit. The lines at 239, 583, 729 and 2614 keV are clearly seen together with the single and double escape peaks of the 2614 keV line at 2100 and 1590 keV respectively. The 860 keV line is somewhat less evident than those already mentioned and the presence of the 511 keV line may be inferred from the asymmetric shape of the 583 keV peak. Figure 7 shows the extent of the background, caused predominantly by the 2614 keV line of ThD, on which all the lower energy peaks are superimposed.

${}_{83}^{207}\text{Bi}$ decays by electron capture to ${}_{82}^{207}\text{Pb}$ and there are strong conversion lines at 480 and 974 keV. A source of ${}_{83}^{207}\text{Bi}$ was used throughout this work for the purpose of β channel energy calibration since the β energies used in the angular correlations were typically in the range 250 \rightarrow 350 keV and greater than approximately 1 MeV. Figure 9 shows the conversion electron spectrum of ${}_{83}^{207}\text{Bi}$, and the effect on the electron spectrum of pulses caused by Compton scattering of γ rays in the plastic scintillator. In order to observe the γ Compton spectrum, a

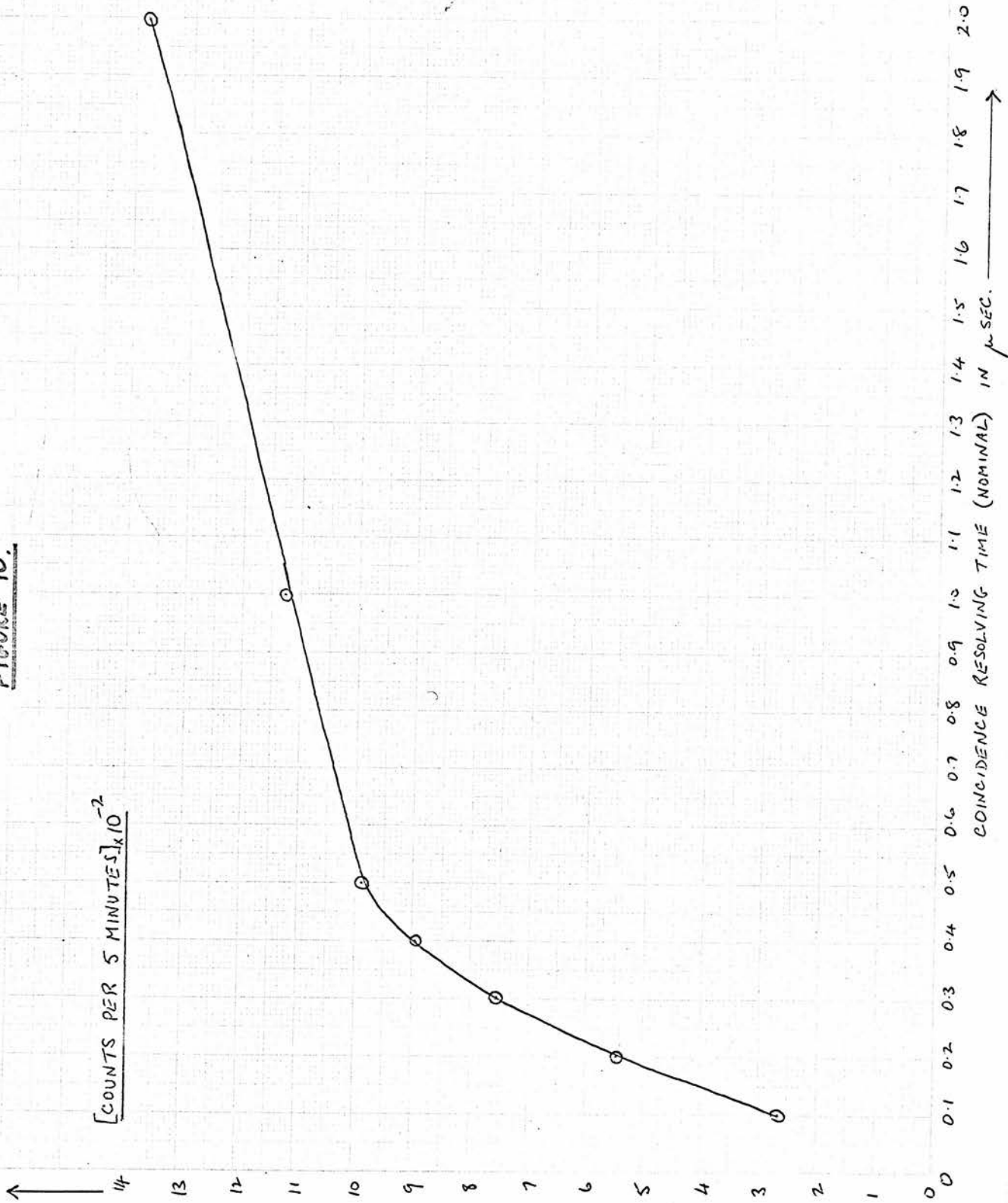
spectrum was recorded with a sufficient thickness of aluminium in front of the source to absorb all the electrons. This was then subtracted from the total $\beta + \gamma$ spectrum. Compton electrons will be generated in the absorber and therefore contribute to the γ background, so the absorber used was no thicker than was necessary to stop the most energetic electrons. To stop a 1 MeV electron, for instance, requires approximately 450 mgm./cm.^2 of aluminium. The γ detector was shielded from all β particles by the combined thicknesses of the chamber wall, the aluminium end of the photomultiplier assembly holder, and the crystal holder. There were therefore no pulses in the γ channel arising from β particles.

Linear plots of particle energy against discriminator bias voltage were obtained for all spectra. No variation of gain with counting rate was observed in the γ channel. This was checked by noting that the 660 keV photopeak and 200 keV back scatter peak produced by a weak source of C_s^{137} lay on the energy calibration line obtained using a very much stronger thorium source. Since the β and γ pulse shapes were very similar, it was assumed that the β energy calibrations derived from the relatively weak Bi^{207} source were still valid at the higher counting rates observed using thorium sources.

3.6 Choice and Measurement of Coincidence Resolving Time

Using a source of E_u^{152} to provide $\beta - \gamma$ coincidences, a plot was made of coincidence counting rate

FIGURE 10.



against the (nominal) resolving time of the coincidence unit. On the basis of this plot, shown in Figure 10, a (nominal) resolving time of 0.5 μ sec. was selected for all later experiments.

The resolving time was measured by the independent source method, which depends on the fact that if the single channel counting rates are N_1 and N_2 per second then the accidental coincidence rate is given by

$$N_A = 2 \gamma N_1 N_2 ,$$

where γ is the resolving time of the coincidence unit. Each counter was provided with a source and lead shielding was placed between the counters such that the source belonging to one of the counters had no effect on the other counter. The single channel rates and the coincidence rate were then recorded over a period of 25 hours. The result was

$$\gamma = 0.56 \pm 0.01 \mu\text{sec.}$$

The variation of coincidence counting rate with delay in each of the two channels was found. In later coincidence experiments, a delay of 0.2 μ sec. was always inserted in the β channel since this value of delay lay in the centre of the region of maximum coincidence counting rate.

3.7 Preparation and Mounting of Sources

The source of E_u^{152} was prepared by dropping a few drops of europium chloride solution onto a 2 mm.

diameter disc of 1 mgm./cm.^2 aluminium foil and evaporating to dryness. This foil was mounted at the centre of a source holder (identical to the one described in section 3.2) by fixing it to a 1 mgm./cm.^2 aluminium backing sheet clamped in the holder. A very tiny smear of grease on the backing sheet sufficed to hold the active foil in position. The active foil was attached to the backing with its active side exposed, which was therefore covered with a small piece of $100 \text{ } \mu\text{gm./cm.}^2$ aluminium foil. The source strength was estimated, from the ratio of true to chance coincidences, to be approximately $100 \text{ } \mu\text{C}$.

Sources of $\text{Th}(B + C + C' + C'' + D)$ were collected electrostatically from a 10 mc parent source of Th^{228} . Th^{228} (half life 1.9 years) decays by α emission to Rn^{220} , an α active gas of 52 second half life. The Rn^{220} α decays presumably leave the resulting Po^{216} atoms ionized and these recoil ions may be collected on aluminium foils, negatively charged with respect to the source. Po^{216} is an α emitter with a 0.16 second half-life and the decay product is the β active Pb^{212} (ThB) which has a half life of 10.6 hours. The decay chain is dominated by the relatively very long half life of the parent and hence Pb^{212} is collected at a constant rate.

The emanating preparation, consisting of hydrated thorium oxide supported on approximately 20 mgm. of hydrated ferric oxide, was placed on a steel tray inside a cylindrical steel pot in a glove box. The thorium sources used in the angular correlation experiments were

collected on 2 mm. diameter discs of 1 mgm./cm.² aluminium foil. The discs were punched from sheets of foil and fixed to the heads of threaded stainless steel buttons by means of a very small smear of grease. Such a source button was then screwed into a brass rod which could be pushed down through a hole in a solid ebonite cylinder so that only the button and source foil emerged at the foot of the cylinder. The ebonite cylinder fitted inside the source pot to expose the source foil just above the emanating preparation. After exposure in the pot, the foil was transferred to the centre of a 2" diameter sheet of 1 mgm./cm.² aluminium foil clamped in the source holder. Again, a very small spot of grease was used to ensure that the active foil did not fall off the backing. The active foil was always placed with the active face in contact with the backing foil so that the source was in the form of a 2 mm. "sandwich" between two 1 mgm./cm.² foils. There was therefore no danger of contamination of the correlation chamber by recoil nuclei following the α decay of ThC and ThC'. Sources of adequate strength were obtained using a negative voltage of 360 V. applied to the brass rod carrying the foil and button, with exposure times varying from three to eight hours.

In order that a correction can be made for source decay during the course of coincidence experiments using thorium sources, it is necessary to know the time (after the exposure has been stopped) which elapses before a

source starts to decay with the 10.6 hour half life of ThB. This time depends on the exposure time itself and can be calculated on the assumption that only ThB atoms are collected on the source foil. In fact there might be some additional ThC" activity caused by contamination of the pot walls and recoil of ThC" atoms following the α decay of ThC. The resultant additional ThC" activity decays with a 3.1 minute half life and may be safely ignored.

The calculation is elementary, but tedious, and proceeds as follows:

Let the disintegration constants in the Th(B+C+C'+C"+D) decay chain be denoted by λ_B, λ_C etc.

$$\text{Then } \lambda_B = \frac{\log_e 2}{10.6} \text{ hours}^{-1} = 0.065 \text{ hours}^{-1}.$$

$$\lambda_C = \frac{\log_e 2}{1.008} \text{ hours}^{-1} = 0.687 \text{ hours}^{-1}.$$

By comparison, λ_C and $\lambda_{C''}$ are huge and terms of the type $\exp(-\lambda_C t)$ and $\exp(-\lambda_{C''} t)$ can be ignored.

Let the source collection time be T hours, beginning at $t = 0$ hours.

$$\text{Then we have } \frac{dN_B}{dt} = n - \lambda_B N_B \quad \text{for } t \leq T$$

in an obvious notation, where n is the constant rate at which ThB atoms are collected. Solving for N_B gives

$$N_B = \frac{n}{\lambda_B} (1 - e^{-\lambda_B t}).$$

For $t \geq T$

$$\frac{dN_B}{dt} = -\lambda_B N_B$$

$$\therefore N_B = {}_0N_B e^{-\lambda_B t}$$

$$\text{where } {}_0N_B = \frac{n}{\lambda_B} (e^{\lambda_B T} - 1) .$$

For ThC we have

$$\frac{dN_C}{dt} = -\lambda_C N_C + \lambda_B N_B \quad \text{for } t \leq T$$

which leads to an expression for N_C as a function of t :

$$N_C = \frac{n\lambda_B}{\lambda_C(\lambda_C - \lambda_B)} \left[e^{-\lambda_C t} - \frac{\lambda_C}{\lambda_B} e^{-\lambda_B t} + \frac{\lambda_C - \lambda_B}{\lambda_B} \right] \quad (1)$$

Solving the equation

$$\frac{dN_C}{dt} = -\lambda_C N_C + \lambda_B N_B \quad \text{for } t \geq T$$

and using (1) to match solutions at $t = T$ finally yields

$$N_C = \frac{\lambda_B}{\lambda_C - \lambda_B} {}_0N_B \left[e^{-\lambda_B t} - \frac{(e^{\lambda_C T} - 1)}{(e^{\lambda_B T} - 1)} \cdot \frac{\lambda_B}{\lambda_C} e^{-\lambda_C t} \right] \quad (2)$$

for $t \geq T$.

The calculation can be extended to give $N_{C'}$ and $N_{C''}$ but this is unnecessary because the dominant terms in $e^{-\lambda_B t}$ and $e^{-\lambda_C T}$ are so very much greater than those in $e^{-\lambda_C' t}$ and $e^{-\lambda_C'' t}$.

If the source is to decay with the half life of ThB, the term containing $e^{-\lambda_C t}$ should be very much less than the one containing $e^{-\lambda_B t}$ in (2). In this work, values of exposure time T were in the range three to eight hours for which the factor



$\frac{e^{\lambda_C T} - 1}{e^{\lambda_B T} - 1} \cdot \frac{\lambda_B}{\lambda_C}$ varies from approximately three to

forty. It was found convenient to expose a source during the day, leave it to decay overnight and use it in an angular correlation experiment the following day. Thus the time t in (2) is approximately 24 hours at least. Putting this value of t in (2) shows that the relative contribution of the ThC half life is only ~ 0.01 to 0.001 % for exposure times ranging from three to eight hours.

A rough calculation of source strength based on the true to chance coincidence rate ratio indicates that sources of $\sim \frac{1}{2}$ mC strength were being collected during an eight hour exposure. This means that the emanating efficiency of the parent source was in the region of 12%.

Eu^{152} has a 13 year half life and corrections for source decay during an experiment lasting a matter of days are negligible.

The thorium and europium sources were supplied by the Radiochemical Centre, Amersham.

CHAPTER 4

4.1 Source Centring

Since the thorium sources decay with a 10.6 half life and had to be renewed every day, it was necessary to use the long lived source of Eu^{152} , identical in size to the thorium sources, to define, once and for all, the position of the chamber lid for which the sources were centred. By using the adjusting screws to move the lid, the Eu^{152} source was centred by trial and error until the γ counting rate was constant to within 1% for the 90° , 135° and 180° positions. The adjusting screws were then locked so that the lid, and therefore the source holder, was always replaced in the same position. The only question was then whether it was possible to deposit the active thorium foils on the centre of the backing foils each time a new source was prepared. With practice this was found to be easy, the centre of the backing foil being marked by a very small spot of grease.

4.2 Experimental Procedure

Coincidence counts and single channel counts were recorded at angles of 90° , 120° , 150° , 180° , the counts at the first three angles being taken on either side of the 180° position and averaged. In the Eu^{152} correlation, only one count was taken in the 180° position for each of two in the other positions and thus less statistical

weight could be attached to this figure than to the others. This fact makes subsequent analysis of data slightly more tedious than need be if the weights are equal and accordingly, in the thorium correlations, two counts were done in the 180° position as the angles were swept through from $90^\circ \rightarrow 270^\circ$. Counting times used in the various runs varied in duration from 5 to 30 minutes per position, but most experiments were performed using the shorter counting time since the effects of gain drifts should be minimized in this way. A typical run lasted approximately 8-9 hours and the β channel energy calibration was checked before and after each run, using the Bi^{207} source. Temperature variations seemed to be the main cause of energy drifts in the two channels and every effort was made to keep the laboratory temperature constant during a run. It was found that the Bi^{207} conversion line at 974 keV maintained its position as determined by the single channel analyser over periods of several weeks, but that there tended to be, overall, a gradual decrease in pulse height caused, perhaps, by steady deterioration of the optical contact. The γ channel energy calibration could be rapidly checked at will by locating the very prominent peak at 239 keV when thorium sources were in use.

When performing angular correlations using the weak line at 729 keV, it was found convenient to determine counting rates at two angles only, namely at 90° and 180° . The information thus gathered is sufficient to

determine the $P_2(\cos \theta)$ coefficient, there being no $P_4(\cos \theta)$ coefficient since the decays are at most first forbidden. Writing the correlation in the form

$$W(\theta) = 1 + a \cos^2 \theta$$

a is referred to as the anisotropy and is clearly given by

$$a = \frac{N(\pi) - N(\pi/2)}{N(\pi/2)}$$

where $N(\pi)$ and $N(\pi/2)$ represent coincidence counting rates at relative counter angles of π and $\pi/2$ respectively. (In fact $N(\pi/2)$ was a sum of counts taken at 90° and 270° , one count in the 180° position being done for each one in the 90° or 270° positions.) If $W(\theta)$ is written as

$$W(\theta) = 1 + \epsilon P_2(\cos \theta)$$

the relationship between a and ϵ is easily seen to be

$$\epsilon = \frac{a}{\frac{3}{2} + \frac{a}{2}} \quad \text{or} \quad a = \frac{\frac{3}{2}\epsilon}{1 - \frac{1}{2}\epsilon} .$$

(In this notation, $\epsilon = A_2(\beta)A_2(\gamma)$).

Angular correlations were carried out in vacuo except in cases where the β energy was $\gtrsim 1$ MeV. The dependence of β channel counting rate on air pressure inside the chamber was checked and there was found to be

a large ($\sim 40\%$) reduction in counting rate as the pressure was increased from $\sim 20\mu$ Hg. to atmospheric pressure when the β channel was set to record particles of energy in the range $230 \rightarrow 360$ keV. When β particles having energies > 800 keV were recorded, the corresponding reduction amounted to some 20% , and for energies > 1 MeV the reduction fell to approximately 3% .

In order to assess the contribution (caused by γ - γ coincidences) to the total coincidence rate, runs were performed with aluminium absorbers in front of the β plastic and of sufficient thickness to stop the most energetic β particles. At first, an absorber in the form of a rectangular sheet was used but it was replaced in later experiments by smaller disc shaped absorbers. The large absorber was obviously cutting out any β particles being scattered from the chamber walls, floor and lid, whereas use of a smaller absorber allows such effects to be subtracted out. The small absorbers were 1" in diameter and placed directly between the source and the β plastic at a distance of approximately 1" from the plastic.

Since the single channel counting rates were recorded, it was possible to calculate the number of accidental coincidences from the relation

$$N_A = 2 \tau N_\beta N_\gamma$$

using the measured value of τ , the coincidence resolving time.

After correction has been made for chance coincidences, the resulting number of genuine coincidences can be corrected for decay of the source. It is evident that such correction must be made after subtraction of chance coincidences, and not before, because the total coincidence rate, N , contains parts which vary differently in time. Thus, the chance rate varies as $\exp(-2\lambda_B t)$ whereas the genuine coincidence rate is a function of source strength only and therefore varies as $\exp(-\lambda_B t)$. Under the conditions of this experiment, either of the single channel counting rates varies as $\exp(-\lambda_B t)$ and so the decay correction can be made by normalizing the genuine coincidences using ratios of singles counts. The number of genuine coincidences obtained in any given count was divided by the total γ count, less background, and multiplied by the first γ count, less background, of a run. The background here referred to is that which is present in the γ counter in the absence of a radioactive source and, since it is constant in time, must be subtracted from the total γ count before the decay correction factors are calculated. It is better to use the γ singles count, rather than the β singles count, for normalization purposes because the γ counter is the moveable one. Any asymmetry in the γ singles count caused by mis-alignment of the source will induce a similar asymmetry in the coincidence count and the normalization procedure therefore serves to correct any such effect.

The background was measured with no source in the chamber for each of the γ -energies used in the angular correlation experiments. A test was made to ensure that the backgrounds in the β and γ counters did not give rise to any genuine coincidences. The β background counting rate was very small (<1 per second) and no genuine coincidences were found.

The γ - γ coincidences, obtained using absorbers, were corrected for the effects of source decay and accidental coincidences in the same way.

The procedure outlined in this section yields a set of coincidence count totals at each of a number of angles, corrections have been made to take account of accidental coincidences, γ - γ coincidences, decay of the source and source mis-alignment. The coincidence counts so corrected can now be used to deduce a value of the anisotropy, a , and the $P_2(\cos \theta)$ coefficient, s .

4.3 Treatment of Data

In analysing the results of an angular correlation experiment it is necessary to fit a set of counting rates y_i , say, determined at angles θ_i to a relation of the form

$$a + \beta \cos^2 \theta_i = y_i \quad (1)$$

In our case, i takes the values 1 to 4 corresponding to angles 90° , 120° , 150° and 180° .

The best values of a and β are obtained from

the "least squares" requirement:

$$\sum_i (\alpha + \beta \cos^2 \theta_i - y_i)^2 = \text{minimum.}$$

Differentiating partially with respect to α and β then yields the normal equations:

$$\left. \begin{aligned} \sum_i \alpha + \beta \sum_i \cos^2 \theta_i &= \sum_i y_i \\ \alpha \sum_i \cos^2 \theta_i + \beta \sum_i \cos^4 \theta_i &= \sum_i \cos^2 \theta_i y_i \end{aligned} \right\} (2)$$

In general, the equations (1) will not necessarily be of equal statistical weight. The observations y_i will have weights w_i , say, where

$$w_i = \frac{1}{\sigma_{y_i}^2} .$$

The y_i may be treated as observations of unit weight if each of the equations of condition (1) is multiplied by the square root of its weight⁽²⁷⁾. In this case the normal equations will be

$$\left. \begin{aligned} \alpha \sum_i w_i + \beta \sum_i w_i \cos^2 \theta_i &= \sum_i w_i y_i \\ \alpha \sum_i w_i \cos^2 \theta_i + \beta \sum_i w_i \cos^4 \theta_i &= \sum_i w_i y_i \cos^2 \theta_i \end{aligned} \right\} (3)$$

The above relations can be expressed neatly in matrix notation. Thus (1) becomes

$$\begin{bmatrix} 1 & \cos^2 \theta_1 \\ 1 & \cos^2 \theta_2 \\ 1 & \cos^2 \theta_3 \\ 1 & \cos^2 \theta_4 \end{bmatrix} \begin{bmatrix} \alpha \\ \beta \end{bmatrix} = \begin{bmatrix} y_1 \\ y_2 \\ y_3 \\ y_4 \end{bmatrix}$$

or $A \begin{bmatrix} \alpha \\ \beta \end{bmatrix} = \underline{y}$.

Multiplying on the left by \tilde{A} (\sim means transpose) gives

$$\tilde{A} A \begin{bmatrix} \alpha \\ \beta \end{bmatrix} = \tilde{A} \underline{y}$$

which are evidently the normal equations (2).

Introducing a square diagonal matrix w having the w_i as its diagonal elements, the normal equations (3) can be written

$$\tilde{A} w A \begin{bmatrix} \alpha \\ \beta \end{bmatrix} = \tilde{A} w \underline{y}$$

or

$$C \underline{a} = \underline{\xi} \tag{4}$$

where $C = \tilde{A} w A$, $\underline{\xi} = \tilde{A} w \underline{y}$ and $\underline{a} = \begin{bmatrix} \alpha \\ \beta \end{bmatrix}$.

The solution of (4) is

$$a_\lambda = \sum_{\gamma} C_{\lambda\gamma}^{-1} \xi_\gamma$$

where $C_{\lambda\gamma}^{-1} = \frac{\text{Cofactor of } C_{\lambda\gamma}}{|C|}$

and $|C|$ is the determinant of the matrix C.

In our case,

$$C = \begin{bmatrix} \sum_i w_i & \sum_i w_i \cos^2 \theta_i \\ \sum_i w_i \cos^2 \theta_i & \sum_i w_i \cos^4 \theta_i \end{bmatrix}$$

and hence

$$\alpha = \frac{1}{|C|} \left(\sum_i w_i \cos^4 \theta_i \sum_i w_i y_i - \sum_i w_i \cos^2 \theta_i \sum_i w_i y_i \cos^2 \theta_i \right)$$

$$\beta = \frac{1}{|C|} \left(\sum_i w_i \sum_i w_i \cos^2 \theta_i y_i - \sum_i w_i \cos^2 \theta_i \sum_i w_i y_i \right)$$

Taking the weights to be equal since this, aside from one case, represents the experimental situation, then

$$\left. \begin{aligned} \alpha &= \frac{1}{|\tilde{AA}|} \left(\sum_i \cos^4 \theta_i \sum_i y_i - \sum_i \cos^2 \theta_i \sum_i y_i \cos^2 \theta_i \right) \\ \beta &= \frac{1}{|\tilde{AA}|} \left(4 \sum_i \cos^2 \theta_i y_i - \sum_i \cos^2 \theta_i \sum_i y_i \right) \end{aligned} \right\} (5)$$

where

$$\tilde{AA} \text{ is the matrix } \begin{bmatrix} 4 & \sum_i \cos^2 \theta_i \\ \sum_i \cos^2 \theta_i & \sum_i \cos^4 \theta_i \end{bmatrix}$$

The existence of an uncertainty in the y_i expressed by $\sigma_{y_i}^2$ will lead to corresponding uncertainties in α and β . σ_α^2 and σ_β^2 can be calculated from equation (5).

Thus, dropping the subscript y_1 in $\sigma_{y_1}^2$ because the measurements are of equal weight,

$$\begin{aligned}
 \sigma_a^2 &= \left[\sum_i \left(\frac{\partial \alpha}{\partial y_i} \right)^2 \right] \sigma^2 \\
 &= \sigma^2 \sum_i \left[\frac{\sum_i \cos^4 \theta_i}{|\tilde{A}A|} - \left\{ \frac{\sum_i \cos^2 \theta_i}{|\tilde{A}A|} \right\} \cos^2 \theta_i \right]^2 \\
 &= \frac{\sigma^2}{|\tilde{A}A|^2} \left[4 \left(\sum_i \cos^4 \theta_i \right)^2 + \left(\sum_i \cos^2 \theta_i \right)^2 \sum_i \cos^4 \theta_i - 2 \sum_i \cos^4 \theta_i \left(\sum_i \cos^2 \theta_i \right)^2 \right] \\
 &= \frac{\sigma^2}{|\tilde{A}A|^2} \left(\sum_i \cos^4 \theta_i \right) \left[4 \sum_i \cos^4 \theta_i + \left(\sum_i \cos^2 \theta_i \right)^2 - 2 \left(\sum_i \cos^2 \theta_i \right)^2 \right] \\
 &= \frac{\sigma^2}{|\tilde{A}A|^2} \left(\sum_i \cos^4 \theta_i \right) \left[4 \sum_i \cos^4 \theta_i - \left(\sum_i \cos^2 \theta_i \right)^2 \right] \\
 &= \frac{\sigma^2 \sum_i \cos^4 \theta_i}{|\tilde{A}A|} \tag{6}
 \end{aligned}$$

A similar calculation yields for σ_β^2 the result

$$\sigma_\beta^2 = \frac{4\sigma^2}{|\tilde{A}A|} \tag{7}$$

These results are in agreement with those of Rose⁽²⁸⁾ who treats the more general case of unequal weights.

The above calculation gives a measure of purely statistical variations of α and β . There is another method of obtaining σ_α^2 and σ_β^2 based on the difference between the measured y_1 and the y_1 calculated from

the values of α and β obtained from the least squares fit. Calling the residuals, that is the values of

$$(y_i)_{\text{exp.}} - (y_i)_{\text{calc.}}, \quad d_i, \quad \text{then it can be shown}^{(27)}$$

that the probable error, S , in any of the y_i is given by

$$S^2 = \frac{\sum_i |d_i|^2}{n - m}$$

where n is the number of measurements and m the number of unknowns. In this case, $n = 4$, $m = 2$.

The analysis leading to equations (6) and (7) can now be carried through again to give values of σ_a^2 and σ_β^2 . Clearly, the only difference is that S^2 replaces σ^2 . The value of S^2 , obtained from a sum of squared residuals, should contain contributions from all sources of error whereas the value of σ^2 is got purely from the counting statistics. A comparison of the relative sizes of σ and S should then indicate the presence or otherwise of any uncertainties other than those arising from statistical fluctuations in the counts.

The value of the anisotropy, a , is

$$a = \frac{\beta}{\alpha}$$

and therefore

$$\frac{\sigma_a^2}{a^2} = \frac{\sigma_\alpha^2}{\alpha^2} + \frac{\sigma_\beta^2}{\beta^2}$$

so that σ_a can be calculated once σ_α and σ_β are known. When calculating σ_α and σ_β , the quantity S^2

was used, since it should encompass errors from all sources. The $P_2(\cos \theta)$ coefficient is given by

$$\epsilon = \frac{a}{\frac{3}{2} + \frac{a}{2}}$$

and it is easily shown that, for small values of a ,

$$\sigma_\epsilon = \frac{2}{3} \sigma_a.$$

In the cases where the anisotropy was measured by taking counts in the $\frac{\pi}{2}$ and π positions only, a is given by

$$a = \frac{N(\pi) - N(\pi/2)}{N(\pi/2)}$$

with the notation of the previous section and

$$\begin{aligned} \sigma_a^2 &= \left(\frac{\partial a}{\partial N(\pi)} \right)^2 \sigma_{N(\pi)}^2 + \left(\frac{\partial a}{\partial N(\pi/2)} \right)^2 \sigma_{N(\pi/2)}^2 \\ &= \frac{\sigma_{N(\pi)}^2}{N(\pi/2)^2} + \frac{N(\pi)^2}{N(\pi/2)^4} \sigma_{N(\pi/2)}^2 \end{aligned}$$

and therefore σ_a^2 can be calculated from the statistical counting errors in $N(\pi)$ and $N(\pi/2)$.

The question arises as to what is the best estimate of the uncertainty in a genuine coincidence total, N_G , which is arrived at by the present means of measuring a total coincidence count, N , and subtracting from this a calculated chance coincidence count N_A . On the assumption that the parent distribution, of which N is a sample, is Poissonian, it is possible to say that such a

measured total count is liable to fluctuations of order \sqrt{N} . It is unlikely that a fluctuation of this order would arise solely from a fluctuation in the genuine coincidence count since N_A , although it is a calculated-quantity, is itself likely to be in error by approximately $\sqrt{N_A}$. The total likely uncertainty, \sqrt{N} , is therefore composed of contributions from N_A and N_G , of order $\sqrt{N_A}$ and $\sqrt{N_G}$ respectively. Since

$$N = N_A + N_G$$

we can assert that

$$\sigma_N^2 = \sigma_{N_A}^2 + \sigma_{N_G}^2 + 2r \sigma_{N_A} \sigma_{N_G}$$

where r is the coefficient of correlation between N_A and N_G . This coefficient must be zero since the N_A and N_G arise from independent Poissonian distributions.

Thus

$$\begin{aligned} \sigma_{N_G}^2 &= \sigma_N^2 - \sigma_{N_A}^2 \\ &= N - N_A \\ &= N_G, \end{aligned}$$

by the particular property of the Poissonian distribution that $\sigma^2 =$ the mean of the distribution. Normalization of the results involved multiplication by numerical factors of the order of unity (typically in the range 1 to 1.5) and calling the factors f_1 , the statistical error in the sum of a number of independent counts was taken as

$$\sigma_{N_G}^2 = \sum_i r_i^2 N_{G_i}$$

It is also possible to claim that, since

$$N_G = N - N_A$$

$$\sigma_{N_G}^2 = \sigma_N^2 + \sigma_{N_A}^2 - 2r' \sigma_N \sigma_{N_A}$$

where r' is the coefficient of correlation between N and N_A . These variables are correlated and a value of r' could be deduced by the standard method⁽²⁷⁾ from the experimental results. This, however, yielded a value of $r' \simeq 1$ in every case simply because the numbers N_A , being calculated from the singles rates, decayed strictly as $\exp(-2\lambda_B t)$ and there was therefore no fluctuation in the calculated values of N_A . Such a situation obviously leads to a high value of r' and, in fact, if $r' = 1$ it is seen that

$$\begin{aligned} \sigma_{N_G}^2 &= \sigma_N^2 + \sigma_{N_A}^2 - 2\sigma_N \sigma_{N_A} \\ &= N + N_A - 2\sqrt{NN_A} \text{ on the assumption} \\ &\quad \text{of Poissonian distributions} \\ &= N_G + 2(N_A - \sqrt{N_A^2 + N_A N_G}) \\ &< N_G \end{aligned}$$

It seems unlikely that $\sigma_{N_G}^2$ could be less than N_G .

It definitely seems unreasonable, on the other hand, to ignore the correlation completely and state that

$$\sigma_{N_G}^2 = \sigma_N^2 + \sigma_{N_A}^2 = N + N_A .$$

It is interesting to note that when a "compromise" value of $\sigma_{N_G}^2$ was taken as being equal to N , this resulted in values of the parameter $x = \frac{S}{\sigma}$ which were with a single exception, less than unity. This was taken as an indication that the value \sqrt{N} was an overly pessimistic estimate of the uncertainty in N_G and the value $\sqrt{N_G}$ was accordingly adopted for this uncertainty. The values of x derived from the assumption $\sigma_{N_G}^2 = N_G$ are quoted in section 4.5. Such values were, naturally, always greater than those derived using the assumption $\sigma_{N_G}^2 = N$.

The final numerical results of all the correlations performed and a discussion of the meaning of these results is deferred until section 4.5 since it is necessary at this point to discuss some further experimental corrections.

4.4 Geometrical and Other Corrections.

The theoretical angular correlation function $W(\theta)$ is derived on the assumption that point detectors and sources are used. Allowance must therefore be made for the smearing produced, in particular, by the finite size of the detectors. Since the source diameters used in this work (2mm.) are so very much smaller than the chamber diameter (~ 15 cm.) it seems reasonable to neglect finite source size corrections.

The calculation of attenuation of the correlation coefficients caused by finite detector size is fairly simple in this case because the detectors are right cylinders, symmetrical about axes taken through the source of the radiation. If the detectors subtend solid angles Ω_1 , and Ω_2 at the source, the measured angular correlation $W'(\theta)$ is given by

$$\begin{aligned} W'(\theta) &= \sum_k A'_{kk} P_k(\cos \theta) \\ &= \frac{\int d\Omega_1 d\Omega_2 W(\theta) \epsilon_1(\alpha_1) \epsilon_2(\alpha_2)}{\int d\Omega_1 d\Omega_2 \epsilon_1(\alpha_1) \epsilon_2(\alpha_2)} \end{aligned}$$

Here, θ is the angle between the detector axes, θ' the angle between the propagation vectors of the radiations while ϵ_1 and ϵ_2 are the efficiencies of the detectors as a function of the entrance angles α_1 and α_2 measured relative to the detector axes. It can now be shown⁽²⁸⁾ that the measured correlation coefficient A'_{kk} and the theoretical one A_{kk} , (i.e. the one calculated on the assumption of point detectors), are related by

$$A'_{kk} = A_{kk} \frac{C_k(x_1)}{C_0(x_1)} \frac{C_k(x_2)}{C_0(x_2)}$$

where $C_k(x_1)$ is given by

$$C_k(x_1) = \int_{\alpha_1=0}^{\alpha_1=x_1} P_k(\cos \alpha_1) \epsilon(\alpha_1) \sin \alpha_1 d\alpha_1$$

with similar definitions for the other C_k 's. x_1 is the half angle subtended on the front face of detector 1. Knowing the dimensions of the apparatus, the calculation of the $C_k(x)$ would be elementary were it not for the need to consider the efficiency of the detectors as a function of entrance angle. In reference (28) the efficiency is taken to be proportional to $(1 - \exp(-t\tau))$ where $t(\alpha)$ is the distance traversed by the radiation incident on the detector at an angle α to the axis and τ is the absorption coefficient for the particular radiation in the particular detector material. Values of the C_k can be calculated for γ rays in NaI crystals using the tables of reference (29) giving τ as a function of γ ray energy. In fact the calculations of reference (28) show that the factors $\frac{C_k}{C_0}$ are rather insensitive to the value of absorption coefficient. For instance, for a source to crystal distance of 10 cm., the factor $\frac{C_2}{C_0}$ varies from 0.978 to 0.974 for values of τ in the range 0.123 to 40 cm.⁻¹. Taking $\epsilon(\alpha) = 1$ is probably a good approximation for the case of β particles detected in a plastic scintillator and, using this approximation and the measured dimensions of the apparatus used in this work, the correction factor for the β detector, $(\frac{C_2}{C_0})_\beta$ was calculated to be 0.98. The correction factor 0.94 was obtained for the γ detector, again on the assumption that $\epsilon(\alpha) = 1$.

A more refined method of calculating the γ detector correction factor is given by Yates⁽³⁰⁾. His analysis takes into account the fact that it is the photopeak efficiency as a function of entrance angle which should be used in the calculation. The calculations are formidable and have to be carried out by computer using Monte Carlo techniques. Tables of results are given by Yates from which the correction factor appropriate to this experiment can be extracted. The value found is 0.95, surprisingly close to the value 0.94 derived from the crude approximation $\epsilon(\alpha) = 1$.

The factor by which the experimental angular correlation coefficients have to be divided, for purposes of comparison with theory, was taken as $0.98 \times 0.95 = 0.93$.

Further effects requiring consideration are those arising from (a) β back scatter in the plastic scintillator, (b) β scattering in the source and source backing material, (c) the β -inner bremsstrahlung angular correlation, and (d) possible perturbation of the angular correlation.

(a) β back scatter

This is the situation where a β particle of energy E incident upon the plastic scintillator undergoes a scattering process whereby a fraction of the energy, ΔE , is recorded but the β particle escapes from the scintillator with the rest. This gives rise to a distortion of the energy spectrum since the detector

registers too great a number of low energy events. The energy dependence of a $\beta - \gamma$ angular correlation will also be distorted because the excess low energy electrons carry with them the angular correlation of the primary higher energy electrons. The work of Freedman et al. (31) on this topic shows that the correction for back scatter becomes important at energies of approximately $\frac{1}{5} E_{\max}$ and less, E_{\max} being the end point energy of the β spectrum. The energies used in the present work were well above the value $\frac{1}{5} E_{\max}$ and, in any case, no attempt was being made to investigate the energy dependence of the angular correlations. As will be seen, the correlations were of "integral" rather than "differential" type, that is all β particles having energy greater than a certain value were used rather than those having energy in a small range $E \rightarrow E + dE$. Clearly, if, as in these experiments, only the existence of an angular correlation is being sought then the fact that it might be slightly enlarged by the effect discussed here is relatively unimportant compared with cases where the energy dependence is being accurately checked.

(b) Scattering of β particles in the source and source backing material.

On the assumption that the electrostatically collected thorium sources were deposited evenly over the 2mm. diameter aluminium discs, the dominant scattering effect will be caused by the 1 mgm./cm.^2 thickness of the

aluminium backing sheets. Such scattering is difficult to deal with theoretically but the effect may be accounted for in terms of a correction factor c_k such that

$$(A_{kk})_{\text{corrected}} = \frac{(A_{kk})_{\text{uncorrected}}}{c_k}$$

in the usual notation. The factor c_k depends on β energy and on the material and thickness of the source backing and can be obtained from a nomogram given by Gimmi et al. (32). The value of c_k appropriate to these experiments is 0.95 for the lowest β energies employed, rising to 0.99 for β energies greater than 800 keV.

(c) β -bremsstrahlung angular correlation

When a β particle interacts with the Coulomb field of a nucleus, the β particle may lose some energy in the form of γ radiation known as bremsstrahlung. Evidently bremsstrahlung can occur as a result of interaction with the field of the β emitting nucleus or with that of some other nucleus belonging to the backing material or the source holder etc. The two cases are known as internal and external bremsstrahlung. $\beta - \gamma$ coincidences will occur as a result of this effect provided that the bremsstrahlung photon has the appropriate energy to register in the γ channel while the β particle has sufficient energy to be accepted in the β channel. The β -internal bremsstrahlung angular correlation

is strongly peaked at an angle of approximately 20° whereas in the present work no readings were taken at angles less than 90° . The β -external bremsstrahlung events, on the other hand, might be expected to show little or no angular correlation because of the haphazard nature of the scattering processes in source backing, holder, chamber walls etc. Also, unless special measures are taken to avoid it - use of low Z materials - the external tends to swamp the internal bremsstrahlung and the total effect is of the order of a few per cent per disintegration⁽³³⁾. It therefore seems reasonable to ignore bremsstrahlung effects, since only a small fraction of this few per cent, decided by detector efficiencies and solid angles as well as by the energy sharing in the process, will yield genuine coincidences.

(d) Perturbation

There is a possibility that the angular correlations might be perturbed by the action of external magnetic fields on the magnetic dipole moments of nuclei or of electric field gradients on the nuclear quadrupole moments. Such perturbing fields are of unknown magnitude in this case, depending as they do on the physical nature of the source. However, their effect on an angular correlation will not usually be serious unless the life time of the intermediate state is much greater than $\sim 10^{-12}$ seconds⁽¹¹⁾.

Some assistance in assessing the probable effect of perturbations of $\beta - \gamma$ angular correlations is given by the $\alpha - \gamma$ angular correlation work of Horton⁽⁴⁸⁾, who

used sources of thorium active deposit similar in collection and construction to those used in the present work. The high energy (perhaps as much as a few hundred keV) nuclear recoil following α disintegration makes it more probable that an $\alpha - \gamma$ angular correlation will be perturbed than a $\beta - \gamma$ angular correlation (where the nuclear recoil energy is \sim a few eV at most in the cases here considered), provided that the life times of the intermediate states are comparable in the two cases. Horton's angular correlation was performed using a cascade of spin sequence 1 - 4 - 5, with an intermediate level life time of approximately 10^{-10} seconds. He concluded, on the basis of the theory of Alder⁽⁷¹⁾, that the reduction in anisotropy was small. This came about largely on account of the high intermediate spin value since it happens that the anisotropy of sequences such as 1 - 4 - 5 is relatively insensitive to changes in population of the magnetic substates of the intermediate level. It therefore seems reasonable to neglect perturbations in the $\text{ThC}'' \rightarrow \text{ThD}$ $\beta - \gamma$ angular correlation where the intermediate spin value is 5 and the life time of the state $\sim 10^{-10}$ seconds⁽⁷²⁾.

Turning now to the $\text{ThC} \rightarrow \text{ThC}'$ correlation, the life time of the 729 keV level on the single particle estimate is 4×10^{-11} seconds. The life time has also been calculated by Bohr and Mottelson⁽⁷³⁾ on the basis of the branching ratio between the long range α particles and 729 keV γ rays from the level. The result is

TABLE I.

	γ RAY ENERGY (keV)	β PARTICLE ENERGY (keV)	ABSORBER	VACUUM	COUNTING TIME (MINS)	ϵ .
1.	239 (ThC)	140 \rightarrow 160	LARGE	YES	10	0.02 ± 0.02 .
2.	"	110 \rightarrow 160	"	"	"	-0.007 ± 0.003 .
3.	"	250 \rightarrow 350	SMALL	"	"	-0.006 ± 0.01
4.	"	"	"	NO	5	-0.04 ± 0.03
5.	"	"	"	YES	"	-0.03 ± 0.02
6.	"	"	"	"	"	0.015 ± 0.01
*7.	"	"	"	"	"	-0.002 ± 0.01
*8.	729 (ThC') + BACKGROUND.	> 800	"	"	"	0.019 ± 0.014
*9.	BACKGROUND.	> 800	"	"	"	0.04 ± 0.02
*10.	729 (ThC')	> 800	"	"	"	0.007 ± 0.02
11.	583 (ThD)	> 1000	"	NO	10	-0.005 ± 0.003 .
12.	583 (ThD)	> 800	"	YES	5	-0.007 ± 0.01
13.	344 (Gd ¹⁵²)	> 1000	LARGE	NO	30	-0.32 ± 0.03 .

* DENOTES CASES WHERE MEASUREMENTS WERE TAKEN AT ANGLES π , $\pi/2$ ONLY.

REFERENCE.	QUOTED VALUE OF ϵ AT CERTAIN β ENERGIES (IN \AA & V).
34	-0.289 ± 0.003 . > 950 (INTEGRAL).
35	-0.314 ± 0.004 @ 950; -0.401 ± 0.011 @ 1400
36	-0.46 ± 0.02 @ 1280.
37	-0.323 ± 0.013 @ 930; -0.374 ± 0.006 @ 1280
38	-0.217 ± 0.013 @ 800; -0.336 ± 0.011 @ 1300
39	-0.335 ± 0.006 @ 920; -0.388 ± 0.004 @ 1380.
40	-0.282 ± 0.014 @ 770; -0.447 ± 0.013 @ 1350.

TABLE 2.

approximately 6×10^{-12} seconds, which is in agreement with a similar calculation of Emery and Kane⁽⁴⁷⁾. Thus it is evident that the probable life time of the state is in the region where perturbation effects should be small and these are therefore neglected.

4.5 Results of the Angular Correlation Measurements

The shaded portions in the γ spectra of Figures 5, 6 and 7 show the γ channel settings for which the angular correlations were performed. Table 1 gives the numerical results of the correlations, the data having been treated according to the procedure given in the previous three sections. The angular correlation coefficient quoted is s , the $P_2(\cos \theta)$ coefficient.

The E_u^{152} angular correlation was performed for purposes of comparison with other results rather than with a view to adding any information of consequence to this well investigated scheme. The correlation was of integral type, all β particles of greater than 1 MeV energy being used. The value 1 MeV was selected so that coincidences of the type β - unobserved γ ray - 344 keV γ ray did not contribute to the coincidence rate. Reference to Figure 3 shows that the end point of the second most energetic partial β spectrum is at 1040 keV and the number of such triple coincidences recorded should be negligible. The result obtained, number 13 in Table 1, is somewhat higher than the directly comparable result of Bhattacharjee and Mitra⁽³⁴⁾ but later results of these authors⁽³⁵⁾ give a larger value of s . It is sufficient to remark that the value of s obtained in the present

work is not at variance with the results in the literature (references 36 - 40) but that the results quoted in these references do not always agree within the experimental errors. Table 2 shows some results taken from references 34-40.

If the spin assignments in the thorium decay chain of Figure 2 are taken to be correct, the β - 239 keV γ ray cascade occurring in the decay of ThB provides a test of instrumental asymmetry. The intermediate spin value is 0 and there should be no angular correlation, irrespective of the degree of forbiddenness of the β transition. This angular correlation was therefore thoroughly investigated using a variety of β energy ranges, different absorbers and absorber thicknesses, different counting times and with and without evacuation of the correlation chamber. On the basis of the results of these correlations, shown in Table 1, as numbers 1 to 7, it was concluded that future correlations would be best performed using the small absorbers of appropriate thickness, 5 minute counts in each position and with the chamber evacuated. The uncertainties quoted are, with the exception of result 7, those calculated on the basis of the sum of the squared deviations between the theoretical (from the least squares fit) and experimental values of the total count in each position. The quantities S^2 and σ^2 defined in section 4.3 can be compared and, defining the ratio $x = \frac{S}{\sigma}$, a value of x in the region of unity may be taken as an indication

that sources of error other than those of a statistical nature were absent. The ratio x was found to be less than unity in results (2), (3) and (6) of Table 1, slightly greater (≈ 1.3) in result (1) and ≈ 2 in results (4) and (5). The fact that the correlation chamber was not evacuated during the experiment leading to result (4) might give an explanation of the poor result. (This was the single result, referred to in section 4.3, which gave a value of $x > 1$ when the estimate $\sigma_{NG}^2 = N$ was employed.) The reason for the result (5) is not at all obvious. It is interesting to note that when the data of result (2) were normalized using β single channel counting rates rather than γ rates, the value of s increased to -0.018 , the calculated uncertainty remaining the same as in the γ corrected case. This shows the corrective effect of γ normalization in annulling false anisotropy caused by source mis-alignment. The conclusion drawn from these results is that the angular correlation is isotropic within the available experimental accuracy. The β -conversion electron angular correlation has been performed by Siegbahn⁽²⁶⁾ and this experiment also gave a null result. The fact that the conversion electrons rather than the 239 keV γ quanta were employed does not, of course, alter the theoretical prediction of an isotropic correlation if the intermediate spin value is zero.

The 239 keV line is superimposed on the Compton backgrounds of many lines in the thorium spectrum and

there will inevitably be coincidences between this Compton background and the low energy β particles used in the $\beta - 239$ keV γ angular correlation. Reference to Figure 6 gives an indication of the intensity of the 239 keV peak relative to this background. It is of the order of 15 : 1 . The only part of the γ spectrum which showed a measurable $\beta - \gamma$ anisotropy was the background caused by the 2.614 MeV γ ray and there were apparently too few coincidences arising from this source to produce an observable effect on the $\beta - 239$ keV γ correlation, unless, of course, the effect was being cancelled by an opposite effect from other Compton distributions. This is unlikely because, as will be seen, the other γ rays examined (583 and 729 keV) showed no detectable $\beta - \gamma$ anisotropy and hence their Compton backgrounds should show none.

The angular correlation performed using the 729 keV γ ray of ThC' used β particles of energy greater than 800 keV. The integral rather than the differential form of correlation was attempted because the fraction of β decays leading to the 729 keV level of ThC' is only some 8% of the total β branch of the ThC β decay. The energy 800 keV was selected because the partial β spectrum of next highest energy leads to a level at 1513 keV in the ThC' and has end point energy of 750 keV. Thus, cascades of the type $\beta - \text{unobserved } (\gamma) - 729$ keV γ ray did not contribute to the angular correlation. Figure 7 shows the continuous background arising from the 2.614 MeV γ ray of ThD (there are some other high (>860 keV) energy γ rays which will contribute, but they are

very much weaker than the 2.614 MeV line). An attempt was made to assess the effect of this background by performing an angular correlation using β particles of energy >800 keV in coincidence with a section of the background of the same channel width as that used to define the 729 keV γ ray photopeak in the correlation using that line. The data from this correlation were treated in the way already outlined but an additional correction had to be applied to take into account variations in source strength before the effect of the background on the already determined $\beta - (729 \text{ keV } \gamma \text{ ray} + \text{background})$ correlation could be subtracted out. This correction was achieved by multiplying the results of a day's run by a factor β_1/β_n where β_1 signifies the first 5 minute β channel singles count of the entire run (lasting many days) and β_n the first 5 minute β channel count of the run of day "n". Source collection times were the same from day to day and therefore the values of β_1/β_n were of the order of unity. The factors were taken into account when the statistical uncertainty of any count was being calculated. The result of the two correlations and that of the corrected correlation are given in Table 1 as results 8, 9 and 10. It is seen that the small anisotropy of result 8 can be wholly accounted for by result 9, leading to a null result, 10, for the corrected $\beta - 729 \text{ keV } \gamma$ angular correlation. It was found that the background coincidences made approximately a 30% contribution to the total $\beta - (729 \text{ keV } \gamma + \text{background})$ coincidence rate. The

contribution of the Compton distribution of the 860 keV γ ray of ThD is not allowed for by the above method but it should be small because the Compton edge of the distribution is at 600 keV and the γ channel setting used to register the 729 keV photopeak should therefore encompass a local minimum in the distribution of the 860 keV line.

Angular correlations were performed using the 583 keV line of ThD, in the one case in coincidence with β particles having energies >800 keV and in the other case with those in the range >1 MeV. The results quoted in Table 1 as numbers 11 and 12 show that there was no angular correlation found within the statistical accuracy. By comparing the number of coincidences obtained using the 583 keV line with those obtained using the continuous γ background and taking into account the different channel widths and source strengths employed, it was estimated that the effect of the background would be to introduce, at most, an anisotropy of $\frac{1}{3}$ % . This lies within the range of experimental error. It is, however, apparent from the decay scheme that coincidences of the type β - unobserved γ - 583 keV γ ray are not eliminated by the present choice of β energy. The most important competing cascade, namely β - unobserved 511 keV γ - 583 keV γ , could have been eliminated by setting the β energy selection to pick out β particles of energy >1.3 MeV. This was attempted, but the number of coincidences was very much reduced

and the matter was not pursued in view of the further possibility of interference by the cascade β - unobserved 277 keV γ - 583 keV γ . Correction for the effect of competing cascades can be made⁽¹¹⁾ but the method entails measurement of the β - 511 keV γ ray correlation and this is not feasible with the present detector because the 511 keV line can be barely distinguished as a hump on the lower energy slope of the 583 keV line. It is at least reassuring that the alteration of the relative contribution of the competing cascades brought about by the change in β energy between the two correlations made no observable difference to the result.

Finally, an attempt to repeat the angular correlation reported by Demichelis and Ricci⁽¹³⁾ resulted in failure. These authors claim to have measured the correlation of the extremely weak ($< 0.5\%$) highest energy ThC^{''} \rightarrow ThD β transition and the succeeding 2.614 MeV γ ray. The β channel discriminator was set to record β particles of energy greater than 2.25 MeV and the γ channel was set to record the 2.614 MeV γ ray photopeak. The number of genuine coincidences recorded after a period of one hour was negligible (2 ± 2) and the experiment was considered not to be feasible with sources of the present strength of $\sim 1/2$ mc. Since the source strength quoted in reference (13) was much less than this (45 μ c), it is difficult to imagine what was being observed in the experiment of Demichelis. The background correlation measured in the present work, is, of course,

an extremely complex affair involving literally dozens of events of the type β - unobserved γ or γ cascade - Compton photon of the 2.614 MeV γ ray.

The conclusions drawn from the present measurements may be stated as follows. The β - 239 keV γ ray angular correlation in the decay $\text{ThB} \rightarrow \text{ThC}$ ($\log ft = 5.2$) shows no angular correlation, as does the β - 729 keV γ ray correlation in the $\text{ThC} \rightarrow \text{ThC}'$ decay ($\log ft = 7.8$) or, at least, none large enough to be detected in the present experiment. It is not possible to make a similar statement with as much confidence about the β - 583 keV γ ray correlation in the $\text{ThC}'' \rightarrow \text{ThD}$ decay ($\log ft = 5.7$) but, in the opinion of the author, it is most unlikely that an anisotropy, detectable using the present apparatus, exists.

CHAPTER 5

5.1 The Decay Scheme of the Thorium Active Deposit

Figure 2 shows the details of the decay schemes of ThB and its descendants which are of importance in this work. The reasoning behind the various spin and parity assignments is now summarized.

ThB, ThC' and ThD are even-even nuclei and it may therefore be assumed that they have 0+ ground states. The zero spin value for the ThC' ground state has been experimentally verified in the $\gamma - \alpha$ angular correlation experiment of Cobb⁽⁴¹⁾. No angular correlation was found between the 729 keV γ ray of ThC' and the succeeding ground state to ground state (of ThD) α transition, as would be expected for zero intermediate spin value.

Further information is obtained from internal conversion coefficient measurements. Thus, the 239 keV line of ThC has been determined to be almost certainly pure M1 radiation from the K/L_I and K/L_{II} conversion ratios and from the $L_I : L_{II} : L_{III}$ sub-shell conversion ratios (42), (43), (44), (45), (46). This makes it very likely that either the ground state of ThC has zero spin and the first excited state a spin of unity, or vice versa. The levels must have the same parity. Also, the 729 keV line of ThC' is pure E2 in nature^{(42), (47)}. The first excited level of ThC' must therefore have spin 2 and positive parity. This assignment is also borne out by the observation of long range α particles from this level. As the

final state of the α transition is the $0+$ ground state of ThD, the α decay selection rules limit the possible spin and parity values of the 729 keV level to $-1-$, $2+$, $3-$ etc. (The α particle has zero intrinsic spin and the parity of the angular momentum state of the α particle is therefore $(-)^l$ where l is the orbital angular momentum carried off by the α particle in the transition. Since parity is conserved in the transition, the α particle must carry off an even number of units of angular momentum if the initial and final parities of the nuclear states are the same, and an odd number if they are different. The value of l is decided by the rule

$$|I_i - I_f| \leq l \leq I_i + I_f$$

where I_i and I_f are initial and final nuclear spins. A decay will normally proceed with emission of as little angular momentum as possible, but mixtures are common with l values differing by 2 units). The 40 keV transition between the first excited state and ground state of ThC" is also of M1 nature⁽⁴⁸⁾ and these states must have the same parity and spins the same or differing by 1 unit.

The level scheme of ThD has been suggested by Elliot et al.⁽⁴⁹⁾, ⁽⁵⁰⁾ and verified by Wood and Jastram⁽⁵¹⁾, ⁽⁵²⁾. $\gamma - \gamma$ angular correlations and conversion coefficient determinations were undertaken by these workers to elucidate the decay scheme.

log ft values for the various β transitions have

LOG f_t HISTOGRAM FOR ALLOWED β DECAY.

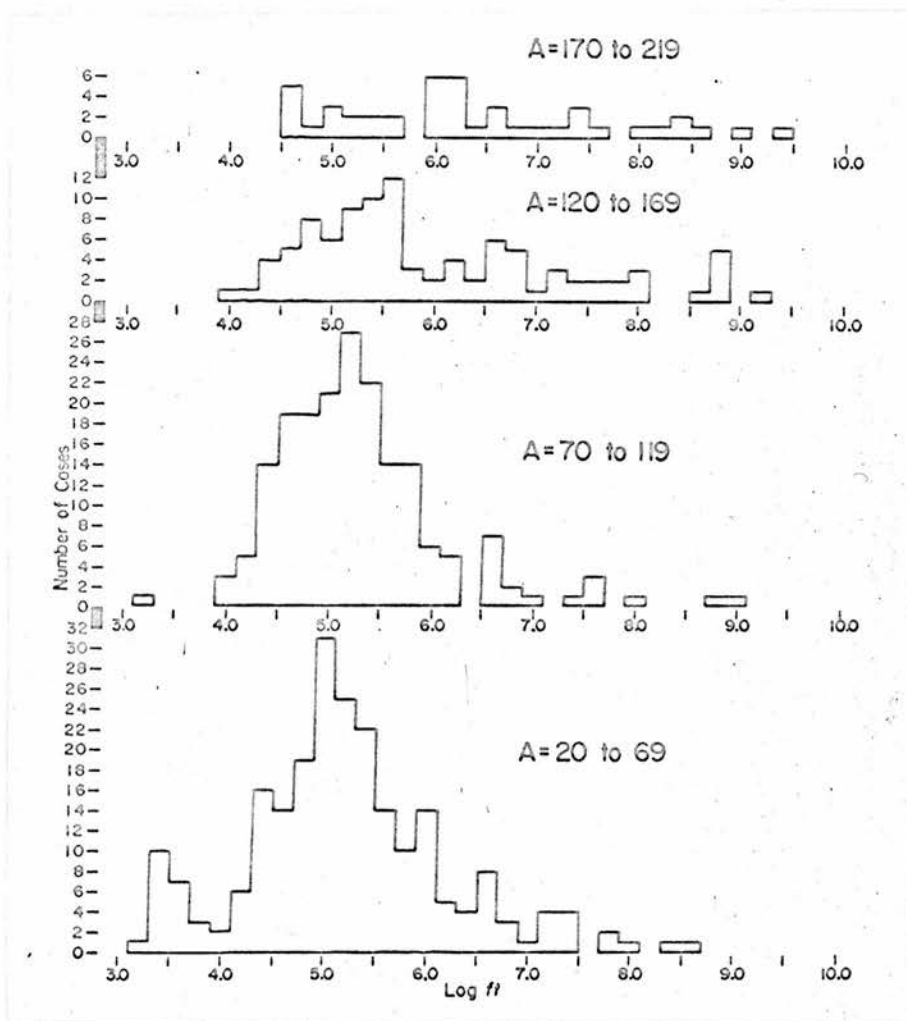


FIGURE II.

LOG f HISTOGRAM FOR
FIRST FORBIDDEN NON-UNIQUE
 β DECAY

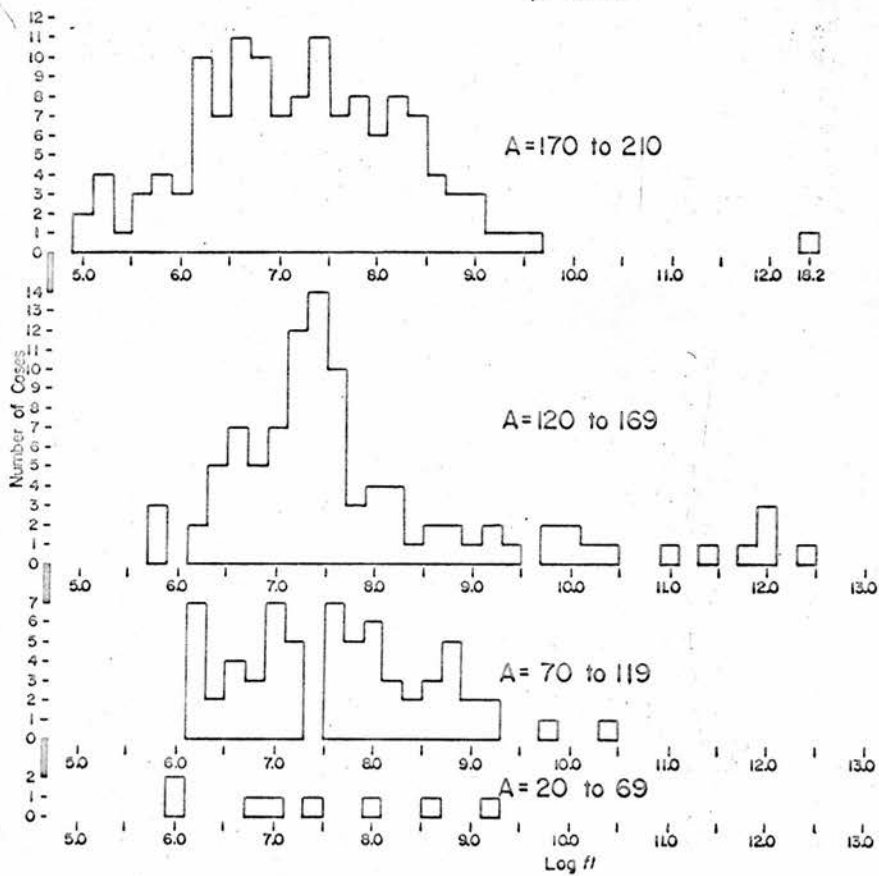


FIGURE 12.

been calculated by a number of workers, for example, by Emery and Kane⁽⁴⁷⁾, and Schupp et al.⁽⁵³⁾. Knowledge of the ground state spins and parities of the odd-odd nuclides ThC and ThC'' would clearly decide the issue of the degree of forbiddenness of the β decays throughout the chain without have recourse to predictions based on log ft values. Figures 11 and 12, histograms from the recent review of Gove⁽⁵⁴⁾, illustrate that there is a trend for log ft values of allowed decays to increase while those of first forbidden decays decrease as the heavier mass regions are approached. Also, many of the anomalously low log ft values of first forbidden decays ($\log ft < 6$) occur near the region of the doubly closed shell nuclide $^{208}_{82}\text{Pb}$ (ThD), although there are cases far removed from this region, e.g. $^{244}_{95}\text{Am}$. It therefore appears doubtful whether the log ft value provides a useful criterion for the determination of degree of forbiddenness as Z increases to values ≥ 82 .

From the measured α intensities in the ThC \rightarrow ThC'' decay, where the ground - ground transition is weaker than the ground - first excited level transition, some conclusions can be drawn as to the probable nature of the ThC ground state. Spin 0 is unlikely because the M1 nature of the 40 keV transition would require the ground and first excited states of ThC'' to have the same spin and parity. If these spins were different, one or other

of the α transitions would be absolutely forbidden under the α selection rules, and if the spins were the same the ground to ground α transition would be expected to be the stronger of the two, which is not the case. Spin 0 would also imply a first forbidden unique or second forbidden β transition in the $\text{ThC} \rightarrow \text{ThC}'$ β branch but the spectrum shape measurements of Burde and Rozner⁽⁵⁵⁾ rule this out. Spin 2 or more is also eliminated by their results. This leaves 1 as being the most likely spin value of the ThC ground state.

Horton⁽⁴⁸⁾ has measured the angular correlation of the 6.05 MeV α particles to the first excited state of ThC'' and the following 40 keV γ ray. This is a crucial experiment and the results are consistent with a spin sequence of 1 - 4 - 5 for the three levels involved. Horton's result is in agreement with the earlier result of Weale⁽⁵⁶⁾. In an α transition between states of spins 1 and 4, the α particle can carry away 3 or 5 units of angular momentum if the parities of the states are different and 4 units only if the parities are the same. In theory, then, the α - γ angular correlation could decide on the relative parities of the ThC and ThC'' states by distinguishing these two cases. Unfortunately, Horton's experiment was not accurate enough to do this and appeal was made to the theory of α fine structure to rule out the case $l_\alpha = 4$. The parities of the states of ThC and ThC'' were therefore determined to be different and the

values 1-, 4+ and 5+ for the spin and parity values in question were selected on the basis of β decay evidence as follows. The spin 1 assignment to the ThC ground state implies spin 0 for the 239 keV excited level because the 239 keV γ ray is pure M1. The ThB ground state \rightarrow ThC 239 keV level β transition has log ft value 5.2 and this suggests a $0^+ \rightarrow 0^-$ transition by analogy with a similar $0^+ \rightarrow 0^-$ transition occurring in the decay of RaD \rightarrow RaE.

If the 1- assignment for the ThC ground state is accepted, then the ground state of ThC" must be 5+. Since the levels of ThD are all well established to be of negative parity, the ThC" \rightarrow ThD β decays must all be first forbidden, as must the ThC \rightarrow ThC' decays because of the E2 nature of the 729 keV γ ray.

Evidence which disagrees with the 5+ assignment to the ThC" ground state is provided by the already quoted angular correlation of Demichelis and Ricci⁽¹³⁾. Their conclusion is that the ground state is 4+ but the present author believes that their experiment is open to doubt.

An alternative scheme, which is not ruled out by any of the measurements referred to above, is one in which the ThC ground state is a 1+ state. The 239 keV level of ThC then becomes 0^+ and the β transition from the ground state of ThB to that level is then allowed, with log ft value in the allowed range. In order to agree with Horton's $\alpha - \gamma$ angular correlations, the ground and first excited levels of ThC" must be given assignments 5- and 4- respectively.

The β transitions in the $\text{ThC}'' \rightarrow \text{ThD}$ decay would then be all allowed with the exception of the weak high energy transition which would be second forbidden. Similarly, the $\text{ThC} \rightarrow \text{ThC}'$ β decays would be allowed. It is clear that this modification of the accepted decay scheme explains immediately the lack of $\beta - \gamma$ angular correlation in the $\text{ThC} \rightarrow \text{ThC}'$ decay.

Comparing the two possible schemes from the point of view of $\log ft$ value, it is seen that the accepted scheme gives some first forbidden decays a low $\log ft$ value, whereas the modified scheme gives some allowed decays a high $\log ft$ value. The modified scheme gives the second forbidden transition of $\text{ThC}'' \rightarrow \text{ThD}$ the rather low $\log ft$ value of 9.2. In view of the general trends shown in the histograms of Figures 11 and 12, there seems little to choose between the two possibilities on the basis of $\log ft$ values.

5.2 Predictions of the Nuclear Shell Model

The nuclear shell model assumes that each nucleon moves independently of the others under the influence of a central potential. The potential well is selected to be intermediate in shape between a square well and a harmonic oscillator well and, provided that a strong spin-orbit interaction is added on, an energy level sequence in the well is obtained which accounts for the magic numbers (75). The energy levels are characterized by values of orbital angular momentum, l , and total angular

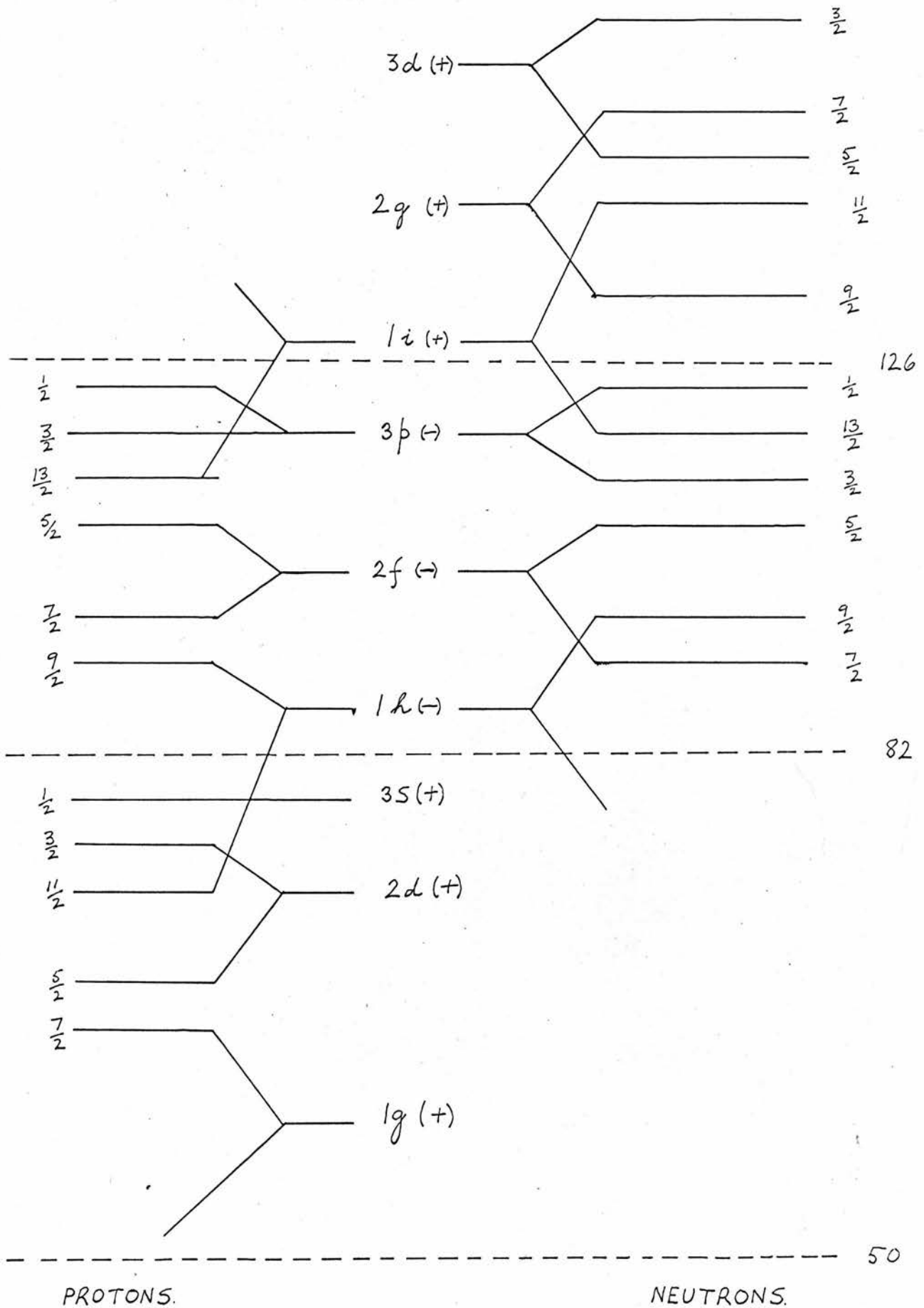


FIGURE 13.

momentum $j = l \pm \frac{1}{2}$. The spectroscopic notation s, p, d, f, g, h etc. for l values of 0, 1, 2, 3, 4, 5 etc. is employed and a number written in front of a configuration, e.g. $3d_{5/2}$ means that this is the third level having $l = 2$, $j = 5/2$. The proton and neutron levels fill independently and a portion of the level scheme proposed by Bergström and Andersson⁽⁵⁷⁾ is shown in Figure 13.

Closed shells occur at nucleon numbers 82 and 126 and ThD therefore has doubly closed shells. When attempting to assign shell model labels to states in this region, the first step must be to determine the single particle states of ${}_{82}^{209}\text{Pb}_{127}$ and ${}_{83}^{209}\text{Bi}_{127}$ and the single hole states of ${}_{82}^{207}\text{Pb}_{125}$ and ${}_{81}^{207}\text{Tl}_{126}$. Once the single particle and single hole configurations have been fixed, one can then proceed to consider two particle nuclei (${}_{83}^{210}\text{Bi}_{127}$, ${}_{84}^{210}\text{Po}_{126}$), two hole nuclei (${}_{82}^{206}\text{Pb}_{124}$, ${}_{81}^{206}\text{Tl}_{125}$) and one particle - one hole nuclei (${}_{81}^{208}\text{Tl}_{127}$, ${}_{82}^{208}\text{Pb}_{126}$). It is of course the excited states of the last named nuclide which will be considered.

Ground state assignments for the first four nuclides mentioned will then be:

${}_{82}^{209}\text{Pb}_{127}$	$9/2+$	$g_{9/2}$	neutron
${}_{83}^{209}\text{Bi}_{126}$	$9/2-$	$h_{9/2}$	proton
${}_{82}^{207}\text{Pb}_{125}$	$1/2-$	$p_{1/2}^{-1}$	neutron
${}_{81}^{207}\text{Tl}_{126}$	$1/2+$	$s_{1/2}^{-1}$	proton

The second column gives the accepted spin and parity assignment,⁽⁷⁶⁾ the third gives the single particle configuration. The superscript "-1" indicates a hole in a closed shell. The ground state configurations of the next set of nuclides mentioned above would then be expected to be, writing the proton configuration first inside the brackets:

${}_{83}^{\text{Bi}}{}_{127}^{210}$	1-	$(h_{9/2}, g_{9/2})$
${}_{84}^{\text{Po}}{}_{126}^{210}$	0+	$(h_{9/2}^2;)$
${}_{82}^{\text{Pb}}{}_{124}^{206}$	0+	$(; p_{1/2}^{-2})$
${}_{81}^{\text{Tl}}{}_{125}^{206}$	0-	$(s_{1/2}^{-1}; p_{1/2}^{-1})$
${}_{81}^{\text{Tl}}{}_{127}^{208}$	5+	$(s_{1/2}^{-1}; g_{9/2})$

It is argued by Carter et al.⁽⁵⁸⁾ and by Lane and Pendlebury⁽⁵⁷⁾ that shell model calculations cannot produce a 3-state low enough in energy to be interpreted as the 3- level of ${}_{82}^{\text{Pb}}{}_{126}^{208}$ and it is concluded that the level may result from a surface vibration of the octopole type.

The ground state of Bi^{210} (RaE) is believed to have spin 1-.⁽⁷⁶⁾ According to Elliot and Lane⁽⁶⁰⁾ and Lee-Whiting⁽⁶¹⁾, the $(h_{9/2}, g_{9/2})$ configuration is not capable of giving a 1- ground state, but the configuration $(h_{9/2}, i_{11/12})$ can do so. The ground state configuration of ${}_{83}^{\text{Bi}}{}_{129}^{212}$ (ThC) might then be $(h_{9/2}, i_{11/12}^3)$ to give a 1- state, the extra two neutrons presumably

coupling to give zero spin. B_1^{214} also has a ground state of 1^- .

More recent theoretical considerations (Spector⁽⁶⁵⁾, Kim and Rasmussen⁽⁶⁶⁾, Mello and Flores⁽⁶⁷⁾), have, however, demonstrated that the $(h_{9/2}, g_{9/2})$ configuration can give a 1^- ground state for RaE. Inversion of the 1^- state with the 0^- ground state expected from this configuration can be obtained both by configuration mixing using excited single particle states of the rigid core and by inclusion of a tensor interaction between the proton and neutron outside the core. Tensor forces were neglected in previous work on the assumption that the effects produced would be small and might be simulated by an effective central force. The RaE results show that this is not always true and that high J configurations with parallel or anti-parallel alignment of angular momenta can experience appreciable tensor effects. The ground state configuration $(h_{9/2}, g_{9/2}^3)$ might then apply to ThC, leading again to a 1^- state.

Thus the shell model evidence points to a 1^- assignment for the ground state of ThC. The level diagram of Figure 13 shows that the proton outside the closed shell is almost certainly in a negative parity state, the nearest positive parity state being $i_{13/2}$. Similarly, the excess neutrons seem certain to be in positive parity states and it is therefore not possible to predict a 1^+ ground state without postulating an $i_{13/2}$ state for the odd proton. Such an assignment seems very unlikely in

view of the well established $9/2$ - ground state of Bi^{209} .

The ground state $(s_{1/2}^{-1}; g_{9/2})$ configuration of ThC'' was predicted by Pryce to form a doublet with spins $5+$ and $4+$. This agrees with Horton's angular correlation result⁽⁴⁸⁾. Measurement of the lifetime of the 40 keV level of ThC'' adds validity to such an assignment because the result $\tau_{\gamma} = (2.06 \pm 0.29) \times 10^{-10}$ seconds⁽⁶³⁾ means that this is an example of an enhanced (over the single-particle estimate) M1 transition. The vast majority of M1 transitions are slower than the single particle estimate⁽⁵⁴⁾. It appears, then, that the ground and first excited states of ThC'' belong to the same configuration (the energy degeneracy being removed by the interaction of the two odd nucleons) because it is necessary to have the contributions from as many particles as possible adding coherently to produce a fast transition. De-Shalit⁽⁶⁴⁾ has calculated the life time of M1 transitions between certain configurations of states for this case and the only configurations used which gave agreement between the theoretical and experimental life times were

$$(s_{1/2}^{-1}; g_{9/2}) \text{ giving } \tau_{\gamma} = 1.8 \times 10^{-10} \text{ seconds with } 5+ \text{ and } 4+ \text{ levels, and}$$

$$(s_{1/2}^{-1}; i_{11/12}) \text{ giving } \tau_{\gamma} = 2.5 \times 10^{-10} \text{ seconds with } 6+ \text{ and } 5+ \text{ levels.}$$

If the second possibility is discarded on the basis of the $\alpha - \gamma$ angular correlation⁽⁴⁸⁾, then the first result

is a very strong argument in favour of the $(s_{1/2}^{-1} ; g_{9/2})$ configuration.

In order to obtain negative parity states of ThC", the proton hole would have to be $h_{11/2}$ instead of $s_{1/2}$, and the Tl²⁰⁷ ground state assignment of $1/2^-$ is a strong argument against this.

The foregoing shell model discussion definitely indicates that, whatever the precise configurations may be in the region of the doubly closed shells (and there may be considerable mixing of configurations), it seems most improbable that the ground states of Bi²¹² and Tl²⁰⁸ can have positive and negative parity respectively without a complete recasting of the shell model level scheme. Such alteration would probably introduce difficulties of explanation of even the most simple expected configurations, that is those of the one particle or one hole nuclei.

It is interesting to note, in passing, the similarities between the ThB \rightarrow ThC β decay and that of RaD \rightarrow RaE. In each case there is a strong $0^+ \rightarrow 0^-$ β transition to the first excited state of the daughter and a much weaker transition from ground state to ground state. The ground state transitions in the ThB and RaD decays have been observed by Feather, Kyles and Pringle⁽⁶⁸⁾ and Byrne⁽⁶⁹⁾, respectively. Byrne found difficulty in making shell model assignments to the levels involved because of the assumption of a ground state $(h_{9/2} \quad i_{11/2})$ configuration for RaE. Since RaD (Pb²¹⁰) is expected to

have a (; $g_{9/2}^2$) configuration, the ground state to ground state β disintegration would not be expected to be of observable intensity. The difficulty obviously disappears if the ($h_{9/2}, g_{9/2}$) configuration is accepted. The ground and first excited states of RaE then both have the configuration ($h_{9/2}, g_{9/2}$). It might be reasonable then to suggest that the ground and first excited states of ThC have the configuration ($h_{9/2}, g_{9/2}^3$) with a ground state assignment of (; $g_{9/2}^4$) to ThB making β transitions possible to both the ground and the first excited states of ThC. The strong β decay from ThC to the ground state of ThC' then suggests a ($h_{9/2}^2 ; g_{9/2}^2$) configuration for the ground state of ThC', which is the assignment of Rasmussen⁽⁷⁰⁾.

Although these shell model assignments appear self-consistent, they do not offer any explanation of the variation in log ft value occurring not only between the various β decays of the thorium chain, but even between branches of the same decay. The log ft value of the $0^+ \rightarrow 0^-$ decay of ThB is lower than that of the $0^+ \rightarrow 1^-$ decay as is the case in the RaD \rightarrow RaE β disintegration. One might be tempted to formulate an empirical rule that $\Delta I = 0$ spin changes are in some way favoured, but this is seen to break down immediately for one of the ThC'' \rightarrow ThD branches. It has been shown by Damgaard and Winther⁽⁷⁴⁾ that low log ft values can be predicted for some first forbidden transitions by taking rigorous account of finite nuclear size effects, but there must still remain

difficulties of explanation of different log ft values to states which might be expected to be members of the same shell model configuration.

There appears at present to be no satisfactory theoretical explanation of such anomalously low log ft values. It is sometimes claimed that such decays are somehow analogous to the mirror transitions of low Z nuclei. In the latter case a particularly good overlap of initial and final state wave functions is brought about by the fact that the β decay merely causes an exchange of proton and neutron numbers in the two participating nuclei. Such claims should surely be treated with some reserve, for there is no guarantee that the shell model configurations remain pure after the addition of only a very few nucleons outside the closed shells.

5.3 Conclusions

No measurable angular correlation has been found for the $\beta - \gamma$ cascades of the thorium active deposit which have been studied. The null result of the $\text{ThB} \rightarrow \text{ThC}$ cascade may be accepted as a corroborative piece of evidence in favour of the 0^- assignment to the 239 keV excited state of ThC . In the opinion of the author, the lack of correlation in the $\text{ThC} \rightarrow \text{ThC}'$ decay is not sufficient evidence to warrant acceptance of an alternative decay scheme of the type mentioned in section 5.1. Admittedly, the null result reported for the $\text{ThC}'' \rightarrow \text{ThD}$ transition is only tentative, but even if it were presented

on much stronger grounds this would not justify an allowed assignment to the β decays in the face of the shell model arguments already put forward.

It should be stressed that the order of magnitude estimate of $A_2(\beta)$ quoted as $\frac{1}{\xi}$ (with $\xi \simeq 15$ for the decays in question) is merely a guide as to the expected size of the correlation. The full expression for $A_2(b)$ contains combinations of the matrix elements contributing to the decay and so long as these matrix elements remain uncalculable (as they are at present), one cannot be too surprised at the non-appearance of an angular correlation.

The lack of correlation in the present experiments could be a result of the integral nature of the measurements. The contribution to an integral correlation at any given β energy is weighted by the β spectrum intensity at that energy. The lower energy portions of the spectrum, where the correlation would be smallest, therefore receive the greatest weights and their contribution might obscure a possible small correlation occurring near the spectrum end point. Reference to the comprehensive table of angular correlation measurements given by Frauentfelder and Steffen⁽¹¹⁾ shows that this happened in the first forbidden decays of Sb^{122} and Au^{198} where differential correlations showed an anisotropy, but integral ones did not. The table also shows zero differential angular correlations in the first forbidden decays of As^{74} , Ce^{141} , Hg^{203} , Nd^{147} and Au^{199} , having log ft values 7.5, 6.9, 6.4, 7.0 and 6.0 respectively. It is notable that

Hg²⁰³ and Au¹⁹⁹ have high Z values and somewhat low log ft values, in fact the lowest out of a total of 30 quoted measurements.

Thus the null results of the present investigation are not without precedent. It would be of interest to study the $\beta - \gamma$ angular correlations of as many as possible of those first forbidden decays which have comparatively low log ft values to discover whether or not there is an observable decrease of angular correlation coefficient with decreasing log ft value of the β decays.

ACKNOWLEDGEMENTS

I am grateful to Professor N. Feather, F.R.S., for making available the facilities of his laboratory.

I am indebted to Mr. J. Kyles, O.B.E., M.A., F.R.S.E., who suggested this topic of research, for many helpful discussions concerning most aspects of this work.

My thanks go to the ex-head of the workshop, Mr. A. Headridge, and his staff, for their assistance in constructing the apparatus. The electronic equipment was very ably serviced by Mr. C. McCanna and his assistants, to whom I am most grateful.

Receipt of a maintenance grant from the Science Research Council during the first year of this work is acknowledged with thanks.

Finally, I thank my wife for all her help.

APPENDIX

Some typical tables of results.

TABLE A1.

β SINGLES	γ SINGLES	N	N _A	N _G	DECAY CORRECTION FACTOR	N _G CORRECTED
878917	45487	136	64	72	1	72
373635	45134	120	63	57	1.008	57
365531	44990	123	61	62	1.011	63
358048	44638	125	60	65	1.019	66
352679	44056	98	58	40	1.033	41
846734	43538	107	56	51	1.045	53
341266	43207	107	55	52	1.054	55
333781	42436	113	53	60	1.073	64
328720	41871	98	51	47	1.088	51
324687	41362	105	50	55	1.101	61
320548	40963	92	49	43	1.112	48
314663	40752	111	48	63	1.118	70
310529	40453	97	47	50	1.127	56
305668	39665	88	45	43	1.149	49
301147	39358	77	44	33	1.159	38
297792	38936	107	43	64	1.171	75
293231	38354	87	42	45	1.189	54
289066	37687	86	41	45	1.211	54

$\theta = 180^\circ$

γ : 729 keV LINE.

β : >800 keV.

COUNTING TIME = 5 MINUTES.

γ BACKGROUND = 700/COUNT.

TABLE A2.

β SINGLES	γ SINGLES	N	N _A	N _G	DECAY CORRECTION FACTOR	N _G CORRECTED.
376730	45009	120	63	57	1.011	58
368059	44783	115	62	53	1.016	54
362321	44506	113	60	53	1.022	54
355640	44175	137	59	78	1.030	80
348706	43527	124	57	67	1.046	70
343358	42906	112	55	57	1.061	60
337716	42491	101	54	47	1.072	50
331931	41966	105	52	53	1.085	58
327938	41499	113	51	62	1.098	68
322703	41199	106	50	56	1.106	62
315410	40101	114	47	67	1.137	76
313687	40330	99	47	52	1.130	59
308500	40113	98	46	52	1.136	59
304105	39419	83	45	38	1.157	44
298897	38963	94	43	51	1.171	60
296938	38487	86	43	43	1.185	51
290797	37483	90	41	49	1.218	60
286166	37272	78	40	38	1.225	47

$\theta = 90^\circ, 270^\circ$ ALTERNATELY. OTHERWISE AS TABLE A1.

TABLE A3.

β SINGLES	γ SINGLES	N	NA	N _G	DECAY CORRECTION FACTOR	N _G CORRECTED.
551263	19885	73	41	32	0.963	31
544043	19488	73	40	33	0.983	32
536817	19362	72	39	33	0.990	33
533022	19101	69	38	31	1.004	31
525214	18788	64	37	27	1.021	28
517723	18741	56	36	20	1.023	20
511344	18384	69	35	34	1.043	35
501405	17809	71	33	38	1.078	41
492395	17648	57	32	25	1.088	27
485964	17620	57	32	25	1.089	27
476086	17441	34	31	3	1.101	3
469562	17390	58	30	28	1.104	31
463893	17084	70	30	40	1.124	45
456892	16575	53	28	25	1.159	29
450491	16646	67	28	39	1.154	45
443994	16256	39	27	12	1.183	14
437056	15893	47	26	21	1.210	25
431582	15561	44	25	19	1.236	23.

γ : BACKGROUND FROM 2.614 MeV LINE.

γ BACKGROUND \doteq 300 / COUNT. OTHERWISE AS TABLE A1.

TABLE A4.

β SINGLES	γ SINGLES	N	N _A	N _G	DECAY CORRECTION FACTOR	N _G CORRECTED.
552895	19169	71	40	31	1	31
547776	19631	78	40	38	0.976	37
541709	18827	68	38	30	1.018	31
535126	19331	56	39	17	0.991	17
524507	18342	53	36	17	1.046	18
522160	18948	47	37	10	1.012	10
514408	18207	63	35	28	1.054	30
506957	17855	49	34	15	1.075	16
495983	17286	40	32	8	1.111	9
490893	17636	58	32	26	1.088	28
481545	17005	47	31	16	1.130	18
474737	17079	59	30	29	1.125	33
465899	16736	47	29	18	1.148	21
458779	16311	57	28	29	1.179	34
452891	16078	41	27	14	1.196	17
447200	16286	53	27	26	1.180	31
440881	15836	52	26	26	1.215	32
434260	15965	58	26	32	1.205	39

$\theta = 90^\circ, 270^\circ$ ALTERNATELY. OTHERWISE AS TABLE A3.

REFERENCES

1. Dunworth, Rev. Sci. Inst. 11, 167, 1940.
2. Hamilton, Phys. Rev. 58, 122, 1940.
3. Beringer, Phys. Rev. 63, 23, 1943.
4. Good, Phys. Rev. 70, 978, 1946.
5. Goertzel, Phys. Rev. 70, 897, 1946.
6. Brady and Deutsch, Phys. Rev. 72, 870, 1947.
7. Yang, Phys. Rev. 74, 764, 1948.
8. Gardner, Proc. Phys. Soc. A62, 763, 1949.
9. Biedenharn and Rose, Rev. Mod. Phys. 25, 729, 1953.
10. Devons and Goldfarb, Handbuch der Physik 42, 362, 1957.
11. Frauenfelder and Steffen, in α , β , γ Ray Spectroscopy, North Holland, 1965, Edited by K. Siegbahn.
12. Ferguson, Angular Correlation Methods in γ ray Spectroscopy, North Holland, 1965.
13. Demichelis and Ricci, Nuovo Cimento 4, 96, 1956.
14. Brink and Satchler, Angular Momentum, O.U.P., 1962.
15. Dirac, Proc. Camb. Phil. Soc. 25, 62, 1928.
16. ter Haar, Reports on Progress in Physics 24, 304, 1961.
17. Fano, Rev. Mod. Phys. 29, 74, 1957.
18. Fermi, Z. f. Physik 88, 161, 1934.
19. Konopinski and Uhlenbeck, Phys. Rev. 60, 308, 1941.
20. Lee and Yang, Phys. Rev. 104, 254, 1956.
21. Wu et. al., Phys. Rev. 105, 1413, 1957.
22. Konopinski, Annual Rev. of Nuc. Science 9, 99, 1959.
23. Blin-Stoyle and Nair, Advances in Physics 15, 493, 1966.
24. Wiedenmuller, Rev. Mod. Phys. 33, 574, 1961.
25. Davisson and Evans, Rev. Mod. Phys. 24, 79, 1952.

26. Siegbahn, Ark. Fysik 4, 223, 1952.
27. Whittaker and Robinson, The Calculus of Observations, Blackie, 1937.
28. Rose, Phys. Rev. 91, 610, 1953.
29. Davisson } in α , β , γ Ray Spectroscopy, North
30. Yates } Holland 1965. Edited by K. Siegbahn.
31. Freedman et al. Rev. Sci. Instr. 27, 716, 1956.
32. Gimmi et al. Helv. Phys. Acta 29, 147, 1956.
33. Van Lieshout et al. in α , β , γ Ray Spectroscopy, North Holland 1965. Edited by K. Siegbahn.
34. Bhattacharjee and Mitra, Nuovo Cimento 16, 175, 1960.
35. Bhattacharjee and Mitra, Phys. Rev. 126, 1154, 1962.
36. Sunier et al. Nuc. Phys. 19, 62, 1960.
37. Fischbeck and Wilkinson, Phys. Rev. 120, 1762, 1960.
38. Dulaney et al., Phys. Rev. 117, 1092, 1960.
39. Alexander and Steffen, Phys. Rev. 128, 1783, 1962.
40. Sunier, Helv. Phys. Acta 36, 429, 1963.
41. Cobb, Phys. Rev. 132, 1693, 1963.
42. Martin and Richardson, Proc. Phys. Soc. A63, 223, 1950.
43. Martin and Parry, Proc. Phys. Soc. A68, 1177, 1955.
44. Sokolowski et al. Nuc. Phys. 1, 160, 1956.
45. Roetling et al. Nuc. Phys. 20, 347, 1960.
46. Krisiuk et al. Nuc. Phys. 4, 579, 1957.
47. Emery and Kane, Phys. Rev. 118, 755, 1960.
48. Horton, Phys. Rev. 101, 717, 1955.
49. Elliot et al. Phys. Rev. 93, 356, 1954.
50. Elliot et al. Phys. Rev. 94, 795, 1954.
51. Wood and Jastram, Phys. Rev. 100, 1237, 1955.
52. Wood and Jastram, Nuc. Phys. 32, 411, 1962.

53. Schupp et al. Phys. Rev. 120, 189, 1960.
54. Gove, in Nuclear Spin-Parity Assignments, Academic Press, 1966. Edited by N.B. Gove.
55. Burde and Rozner, Phys. Rev. 107, 531, 1957.
56. Weale, Proc. Phys. Soc. A68, 35, 1955.
57. Bergström and Andersson, Ark. Fysik 12, 415, 1957.
58. Carter et al. Phys. Rev. 120, 504, 1960.
59. Lane and Pendlebury, Nuc. Phys. 15, 39, 1960.
60. Elliot and Lane, Handbuch der Physik 39, 241, 1957.
61. Lee-Whiting, Phys. Rev. 97, 463, 1955.
62. Pryce, Proc. Phys. Soc. A65, 773, 962, 1952.
63. Sevier, Nuc. Phys. 61, 601, 1965.
64. De-Shalit, Phys. Rev. 105, 1531, 1957.
65. Spector, Nuc. Phys. 40, 338, 1963.
66. Kim and Rasmussen, Nuc. Phys. 47, 184, 1963.
67. Mello and Flores, Nuc. Phys. 47, 177, 1963.
68. Feather, Kyles and Pringle. Proc. Phys. Soc. 61, 466, 1948.
69. Byrne, Thesis, University of Edinburgh, 1962.
70. Rasmussen, Nuc. Phys. 44, 93, 1963.
71. Alder, Helv. Phys. Acta, 25, 235, 1951.
72. Lindskog et al. in α , β , γ Ray Spectroscopy, North Holland, 1965. Edited by K. Siegbahn.
73. Bohr and Mottelson, Dan. Mat. Fys. Medd. 27, No. 16, 1953.
74. Damgaard and Winther, Nuc. Phys. 54, 615, 1964.
75. Mayer and Jensen, Elementary Theory of Nuclear Shell Structure, Wiley, 1955.
76. Strominger et al., Rev. Mod. Phys. 30, 585, 1958.